

# Approaches to spatial confounding in geostatistics

Brian Gilbert, Abhirup Datta, Joan A. Casey  
and Elizabeth L. Ogburn

*Abstract.* Over the past few decades, addressing “spatial confounding” has become a major topic in spatial statistics. However, the literature has provided conflicting definitions, and many proposed solutions do not address the issue of confounding as it is understood in causal inference. We give a clear account of spatial confounding as the existence of an unmeasured confounding variable with a spatial structure. Under certain conditions, including the measurability of the confounder as a function of space, we show that spatial covariates (e.g. latitude and longitude) can be handled by existing causal inference estimation procedures. We focus on “double machine learning” (DML), a procedure in which flexible models are used to regress both the exposure and outcome variables on confounders to arrive at a causal estimator with favorable robustness properties and convergence rates. These models avoid restrictive assumptions, such as linearity and effect homogeneity, which are typically made in spatial models and which can lead to bias when violated. We demonstrate the advantages of the DML approach analytically and via extensive simulation studies. We apply our methods and reasoning to a study of the effect of fine particulate matter exposure during pregnancy on birthweight in California.

*Key words and phrases:* spatial statistics, causal inference, spatial confounding, double machine learning.

## 1. INTRODUCTION

For most of its history the field of spatial statistics has been concerned primarily with spatial process models, where the goal is prediction and interpolation of a spatially varying outcome  $Y$  (e.g. [26], [2], [74], [63], [13]). However, there is now increasing interest in making inferences about the causal effect of an exposure  $X$ , possibly also spatially varying, on  $Y$ . For the most part, researchers interested in such causal effects have relied

on existing spatial models and attempted to clarify when these spatial models can support valid causal inferences [50, 36, 61, 37]. A few papers have drawn from causal inference theory and methods to propose adaptations to existing spatial models [51, 61, 32, 49, 67]. These papers largely deal with *spatial confounding*: unmeasured variables that are thought to possess a spatial structure and influence both the exposure and outcome of interest.

We explore how spatial models relate to the identification assumptions commonly used in causal inference. The motivation for spatial models arises from “Tobler’s First Law of Geography” which states that “everything is related to everything else, but near things are more related than distant things” [68]; spatial models are regression models that take into account the similarity of spatially proximate observations.

We provide a clear statistical framework to understand spatial confounding for geospatial (continuous or point-referenced) data and thoroughly investigate the causal assumptions required for identification of causal effects in its presence. We review existing methods for causal inference in spatial settings and demonstrate conceptually and empirically how some established methods to allevi-

---

Brian Gilbert is Ph.D. student, Department of Biostatistics, Johns Hopkins Bloomberg School of Public Health, Baltimore, MD, USA (e-mail: [bgilber9@jhmi.edu](mailto:bgilber9@jhmi.edu)). Abhirup Datta is Associate Professor, Department of Biostatistics, Johns Hopkins Bloomberg School of Public Health, Baltimore, MD, USA (e-mail: [abhidatta@jhu.edu](mailto:abhidatta@jhu.edu)). Joan A. Casey is Assistant Professor, Department of Environmental Health Sciences, Columbia Mailman School of Public Health, New York, NY, USA (e-mail: [jac2250@cumc.columbia.edu](mailto:jac2250@cumc.columbia.edu)). Elizabeth L. Ogburn (to whom correspondence should be addressed) is Associate Professor, Department of Biostatistics, Johns Hopkins Bloomberg School of Public Health, Baltimore, MD, USA (e-mail: [eogburn@jhu.edu](mailto:eogburn@jhu.edu)).

ate spatial confounding fail to address the problem. We then turn to the application of robust methods that have been extensively studied in the causal inference literature but have, to our knowledge, never been used in the spatial literature. This includes the method of “double machine learning” (DML), in which flexible models are used for regressions of both the outcome and exposure on covariates, and the estimation of a “shift estimand,” or the expected change in population-level outcomes if all individuals’ exposures were shifted by a pre-specified value  $\delta$ . We demonstrate that these methods can improve the efficiency, robustness, and interpretability of inference about causal effect in spatial data. As far as we are aware, this is the first approach to spatial confounding that does not rely on restrictive parametric assumptions (such as linearity, effect homogeneity, or Gaussianity) for both identification and estimation.

In Section 2 we review the standard framework for nonparametric identification of causal effects and propose a rigorous definition of “spatial confounding” that is grounded in causal inference. Section 3 reviews existing methods for spatial causal inference and spatial confounding, with a focus on the assumptions that must be met in order for each method to provide valid causal inferences. In Section 4 we unpack the assumptions that will identify causal effects in the presence of spatial confounding and provide the first fully nonparametric identification results for this setting. We propose shift interventions for spatial causal effects and show how these causal effects can be more interpretable and require weaker assumptions for identification than more typical causal estimands. In Section 5 we demonstrate how flexible machine learning methods can be used in lieu of existing methods for spatial causal inference. These are not limited by parametric assumptions such as effect linearity and homogeneity. These methods are common in the theoretical causal inference literature but we are not aware of them having been used previously in spatial settings. Section 6 is a simulation study demonstrating the fragility of existing methods in the face of violations of parametric assumptions on which they rest and the advantages of DML methods for shift interventions. In Section 7, we analyze a California dataset regarding the effect of fine particulate matter ((particulate matter  $\leq 2.5 \mu\text{m}$  in diameter,  $\text{PM}_{2.5}$ ) exposure during pregnancy on birthweight using the reasoning and methods developed in the paper. Section 8 concludes.

## 2. SPATIAL AND CAUSAL CONFOUNDING

The term “spatial confounding” is frequently used to explain why point estimates from spatial models may be different from point estimates from naive models like ordinary least squares (OLS) that do not use any spatial information. However, this term has rarely been defined explicitly, and we have identified at least four phenomena that are sometimes referred to as “spatial confounding”:

1. **Omitted confounder bias:** The existence of an unmeasured confounding variable with a spatial structure (i.e., an unmeasured variable that obeys Tobler’s law and that influences both the exposure and the outcome) [e.g. [61]].
2. **Random effect collinearity:** The change in fixed effect estimates that may come about when spatially-dependent random effects added to a regression model are collinear with the covariates [e.g. [36]].
3. **Regularization bias:** The finite-sample bias of methods that use flexible regression functions like splines or Gaussian processes (GP) to control for an unknown function of space [e.g. [22]].
4. **Concurvity:** The difficulty of assessing the effect of an exposure which is, or is close to, a smooth function of space, if an arbitrary smooth function of space is also included in a regression model [discussed in [55, 50]].

The first of these notions of spatial confounding is consistent with standard causal definitions of confounding and is the definition that we will use throughout. The others are statistical notions that need not be related to causal confounding. Furthermore, as we explain below, random effect collinearity need not be considered a problem, since correctly accounting for confounding should in general entail a change in effect estimates. In the rest of this section we will review causal inference perspectives on confounding and discuss how they apply specifically in spatial settings.

### 2.1 A brief review of causal inference concepts

Causal effects are typically defined in terms of *potential outcomes* or *counterfactuals*. Let  $Y$  be an outcome and  $X$  an exposure of interest. A potential or counterfactual outcome  $Y(x)$  is the outcome that would have been observed if, possibly contrary to fact, the exposure had been set to value  $x$ , holding all else constant. Typically only one potential outcome is observed for each unit; the fact that only one of two (if  $X$  is binary) or infinite (if  $X$  is continuous) potential outcomes can be observed is known as the “fundamental problem of causal inference” [57]. The challenge, then, is to make inferences about the expectation or distribution of potential outcomes despite not being able to fully observe them.

The distribution  $\mathcal{P}_{full}(Y(x), X, C)$ , where  $C$  is the set of measured covariates, is known as the *full data distribution*; it is the joint distribution of covariates, exposure, and the (partially unobserved) potential outcomes. The *observed data distribution*  $\mathcal{P}_{obs}(Y, X, C)$  is the joint distribution of covariates, exposure, and the observed outcome. We say that a causal estimand of interest (typically a functional of the full data distribution) is *identified* in a causal model if it can be written as a functional of the observed data distribution.

For the rest of this section we will restrict our attention to the identification of the causal estimand  $E[Y(x)]$ . If this expectation is identified then so are causal effects such as  $E[Y(x)] - E[Y(x')]$ , i.e., the expected change in outcomes if  $X$  were set to  $x$  compared to  $x'$ .  $E[Y(x)]$  is not identified from the observed data in general, but it can be identified under the following assumptions:

A1 (Consistency). There are not multiple versions of exposure beyond those recognized by the model: if  $X_i = x$ , then  $Y_i = Y_i(x)$

A2 (Positivity or overlap). There is positive probability of each exposure at every level of covariates:  $0 < P(X = x|C = c)$  for all  $x$  in the support of  $X$  and  $c$  in the support of  $C$  if  $c \in \text{supp}(C)$  and  $x \in \text{supp}(x)$ , then  $(x, c) \in \text{supp}(X, C)$ .

A3 (Conditional ignorability or no unmeasured confounding). Potential outcomes are independent of exposure assignment conditional on observed covariates: for all  $x$  in the support of  $X$ ,  $Y(x) \perp X|C$ .

Confounding is present when ignorability does not hold marginally, that is  $Y(x) \not\perp X$ , and a covariate  $C$  may be referred to as a confounder if conditioning on it helps to achieve ignorability [71]. Unmeasured confounding is present if ignorability holds conditional on  $C, U$  for some measured confounders  $C$  and unmeasured confounders  $U$ , but  $C$  alone does not suffice for ignorability to hold. That is, there is unmeasured confounding by  $U$  if  $Y(x) \perp X|C, U$  but  $Y(x) \not\perp X|C$ .

Under assumptions A1-A3,  $E[Y(x)]$  can be identified as follows:

$$(1) \quad \begin{aligned} E[Y(x)] &= E[E[Y(x)|C]] \\ &= E[E[Y(x)|C, X]] \\ &= E[E[Y|C, X = x]] \end{aligned}$$

where the second equality follows from the conditional ignorability assumption, the third from the consistency assumption, and the positivity assumption ensures that the conditioning event has positive probability. The last line is a functional of the observed data alone, known as the *identifying functional*. While these are the typical identifying assumptions in causal inference, other assumptions can also be used to link the full to the observed data distributions. Because these particular identifying assumptions are fully nonparametric, that is they do not place any restrictions on the observed data distribution, we say that  $E[Y(x)]$  is *nonparametrically identified*.

Estimation strategies that use the expression in equation (1) to estimate  $E[Y(x)]$  rely on a correctly specified outcome regression. An alternative identifying expression

allows estimation via *propensity score* estimation instead, where the propensity score is defined as  $P(X = x|C)$ :

$$\begin{aligned} E[Y(x)] &= E[E[Y(x)|C]] \\ &= E\left[E\left[Y(x) \frac{I_{X=x}}{P(X=x|C)} | C\right]\right] \\ &= E\left[E\left[Y \frac{I_{X=x}}{P(X=x|C)} | C\right]\right] \\ &= E\left[Y \frac{I_{X=x}}{P(X=x|C)}\right] \end{aligned}$$

where  $I_{X=x}$  is the indicator that  $X = x$ . The first equality holds by the law of iterated expectations, the second by ignorability and positivity (which ensures that the denominator is non-zero), the third by consistency, and the fourth again by iterated expectations.

## 2.2 Double robustness

Outcome regression and propensity score regression can be combined to generate *doubly robust* estimation strategies that are consistent for  $E[E[Y|C, X = x]] = E\left[Y \frac{I_{X=x}}{P(X=x|C)}\right]$  if either one, but not necessarily both, of the outcome regression and propensity score models are correctly specified. We return to doubly robust estimation in Section 5. Here we review the basic framework in the context of a binary exposure  $X$ .

Let  $f(X, C) = E[Y|X, C]$  and  $e(C) = P(X = 1|C)$ . Assume  $\hat{f}(x, c) \rightarrow_{n \rightarrow \infty} f(x, c)$  and  $\hat{e}(c) \rightarrow_{n \rightarrow \infty} e(c)$ . We hope that  $f = f$  and  $\hat{e} = e$ , but we will explore what happens if only one of the two converges to the truth.

Consider the estimator of  $E[Y(1)]$  given by

$$\hat{\mu}_1 = \frac{1}{n} \sum_{i=1}^n \left( \frac{X_i Y_i}{\hat{e}(C_i)} - \frac{X_i - \hat{e}(C_i)}{\hat{e}(C_i)} * \hat{f}(C_i, 1) \right).$$

Under suitable regularity conditions,

$$\begin{aligned} \hat{\mu}_1 &\rightarrow E\left[\frac{XY}{\tilde{e}(C)} - \frac{X - \tilde{e}(C)}{\tilde{e}(C)} * \tilde{f}(C, 1)\right] \\ &= E\left[\frac{X * Y(1)}{\tilde{e}(C)} - \frac{X - \tilde{e}(C)}{\tilde{e}(C)} * \tilde{f}(C, 1)\right]. \end{aligned}$$

Under the identifying assumptions from Section 2.1, this is equal to

$$E[Y(1)] + E\left[\frac{1}{\tilde{e}(C)} * (X - \tilde{e}(C)) * (Y(1) - \tilde{f}(C, 1))\right].$$

So  $\hat{\mu}_1 \rightarrow E[Y(1)]$  if and only if

$$E\left[\frac{1}{\tilde{e}(C)} * (X - \tilde{e}(C)) * (Y(1) - \tilde{f}(C, 1))\right] = 0.$$

Consider what happens if  $\tilde{e} = e$ . Then

$$\begin{aligned} & E \left[ \frac{1}{\tilde{e}(C)} * (X - \tilde{e}(C)) * (Y(1) - \tilde{f}(C, 1)) \right] \\ &= E \left[ E \left[ \frac{1}{\tilde{e}(C)} * (X - \tilde{e}(C)) * (Y(1) - \tilde{f}(C, 1)) | Y(1), C \right] \right] \\ &= E \left[ E \left[ \frac{1}{e(C)} * (X - e(C)) * (Y(1) - \tilde{f}(C, 1)) | Y(1), C \right] \right] \\ &= E \left[ \frac{1}{e(C)} * (Y(1) - \tilde{f}(C, 1)) * E[X - e(C) | Y(1), C] \right]. \end{aligned}$$

By ignorability, the inner factor  $E[X - e(C) | Y(1), C]$  is equal to  $E[X | C] - e(C) = e(C) - e(C) = 0$ , and therefore the entire expression is equal to zero, regardless of  $\tilde{f}$ .

On the other hand, if  $\tilde{f} = f$ , then

$$\begin{aligned} & E \left[ \frac{1}{\tilde{e}(C)} * (T - \tilde{e}(C)) * (Y(1) - \tilde{f}(C, 1)) \right] \\ &= E \left[ E \left[ \frac{1}{\tilde{e}(C)} * (X - \tilde{e}(C)) * (Y(1) - \tilde{f}(C, 1)) | C, X \right] \right] \\ &= E \left[ E \left[ \frac{1}{\tilde{e}(C)} * (X - \tilde{e}(C)) * (Y(1) - f(C, 1)) | C, X \right] \right] \\ &= E \left[ \frac{1}{\tilde{e}(C)} * (X - \tilde{e}(C)) * E[(Y(1) - f(C, 1)) | C, X] \right] \end{aligned}$$

By ignorability, the inner factor  $E[(Y(1) - f(C, 1)) | C, X]$  is equal to  $E[Y(1) | C] - f(C, 1) = f(C, 1) - f(C, 1) = 0$ . So as before, the estimator is consistent, regardless of  $\tilde{e}$ .

A similar argument applies for  $E[Y(0)]$ . We can consistently estimate expected potential outcomes if *either*  $\tilde{f} = f$  or  $\tilde{e} = e$ . Practically, this means that we only need to correctly specify *either* the outcome model or the propensity score model. Furthermore, the rate of convergence of the doubly robust estimator is typically the *product* of the rates of the convergence of the nuisance estimators, leading to nonparametric *double machine learning* estimators that achieve  $\sqrt{n}$  rates (see Chernozhukov et al. 2018) when both the outcome regression and propensity score models are consistently estimated at rate  $n^{1/4}$ .

### 2.3 Towards a causally informed definition of spatial confounding

We can now recast the first notion of spatial confounding, omitted variable bias due to a spatially varying unmeasured confounder, in more precise terms. If researchers are interested in estimating the causal effect of a (possibly spatially varying) exposure  $X$  on a spatially varying outcome  $Y$ , then we will say that there

is unmeasured spatial confounding if  $Y(x) \not\perp\!\!\!\perp X | C$  but  $Y(x) \perp\!\!\!\perp X | C, U$ , where  $C$  are measured confounders and  $U$  is an unmeasured, spatially varying confounder. That is, ignorability does not hold conditional on measured confounders alone but it does hold with the addition of a spatially varying – but unmeasured – confounder  $U$ . This unmeasured variable might be a concrete quantity, such as noise pollution levels or household income, but in principle it may be an abstract latent variable.

We emphasize the following fundamental fact: in the presence of arbitrary (unstructured) unmeasured confounding, the identification and estimation of causal effects (i.e., the complete elimination of omitted variable bias) is in general not possible. The presence of an arbitrary unmeasured confounder leaves no imprint on the observed data, and therefore the only approach to control for unmeasured confounding or to mitigate unmeasured confounding bias is to make untestable assumptions that create a bridge between the observed data and the unmeasured confounder. With this fact in mind, the presence of spatial confounding may be seen as a blessing rather than a curse, contrasted with unmeasured confounding that has no spatial structure. This is because spatial information may be leveraged to capture some of the variability in the confounder and, possibly, to control for some of the confounding. In this case, it is the assumption of a spatial structure that creates the bridge between the observed data and the unmeasured confounder. As we will see below, existing approaches to spatial confounding typically model unmeasured spatial effects with splines on location or spatial random effects. However, the mere presence of spatial variation in  $U$  does not suffice for these spatial methods to mitigate spatial confounding, because whenever an unmeasured confounder has some variation that is *not* spatially determined it is always possible that confounding is due precisely to the non-spatial variation in  $U$ . In Section 4 we provide formal conditions under which spatial information suffices to control for unmeasured spatial confounding.

## 3. EXISTING APPROACHES TO SPATIAL CONFOUNDING

The methods presented in this section all assume a data generation process where there is residual spatial variation in the outcome beyond what is explained by the covariates and exposure; this variation can be modeled as a fixed or random effect of space. When used for spatial confounding the (sometimes implicit) assumption is that the fixed or random function of space controls for unmeasured spatial confounding. We have identified three assumptions on the data generating process that are commonly made in the existing spatial confounding literature:

1. There exists an unmeasured variable  $U$  which is a *fixed* function of spatial location  $S$ , and  $U$  influences both  $X$  and  $Y$ . If  $S$  is considered random, then  $U$  is random as well, and so we may say that  $U$  and  $X$  are correlated. If  $S$  is considered fixed, then  $U$  is a nonrandom entity that is empirically associated with  $X$ .
2. There exists an unmeasured variable  $U$  which is a *random* function of spatial location, and  $U$  influences both  $X$  and  $Y$ . In this case,  $U$  is correlated with  $X$  whether or not  $S$  is random.
3. There exists an unmeasured variable  $U$  which is a zero-mean random function of spatial location, and  $U$  influences  $Y$ , but not  $X$ . In this case,  $U$  is not a “confounder”, it merely introduces dependence among the outcomes and naive estimators (like OLS) of the effect of  $X$  on  $Y$  are unbiased, although they may be inefficient or be associated with incorrect standard errors.

It is generally not obvious which scientific contexts justify the consideration of fixed or random effects for the locations in the data generation process. In what follows, we will mainly consider case 1; that is, we assume that there exists an unmeasured variable  $U := U(S)$ , which is a fixed function of spatial location  $S$  and influences both  $X$  and  $Y$ . If the locations  $S$  are considered to be sampled randomly, then  $U = U(S)$  is random as well, and so we may say that  $U$  and  $X$  are correlated. If  $S$  is considered fixed, then  $U$  is a nonrandom entity that is empirically associated with  $X$ . Although in some cases the assumption of random sampling of locations may be unreasonable (e.g., if locations are taken on a regular lattice), the distinction between random and fixed sampling of locations may not be crucial since inference may proceed conditional on the selected locations, assuming they are ancillary to the parameters of interest. With minimal loss of generality we will treat  $S$  as random in what follows. Note that the assumption that  $U$  is a fixed function of space in the true data generation process should not be confused with the modeling choice to regress  $Y$  on a random function of space, e.g. using a Gaussian process regression, which may still be a valid estimation strategy (subject to assumptions) in the same way a fixed parameter can be modeled as a random quantity by assigning a prior in a Bayesian setting.

In spatial statistics literature, it is common to model spatial effects as random functions; we see a few reasons for this. First, physical variables are rarely simple or orderly functions of space, and the complexity of real-world confounding surfaces (that is, a confounding variable as a function of two-dimensional spatial location) may be reminiscent of subjective notions of randomness. And second, Gaussian processes, a particular class of random functions, are popular for their theoretical properties,

and they are empirically successful in estimating fixed functions by formally modeling them as random variables. However, there is nothing inherently *random* about the true complex functions or surfaces in most applications. For example, using a Gaussian process to fit topographical elevation does not commit the researcher to any model of how that pattern of elevation came about, or to the view that topographical elevation is a random quantity. Deciding whether to model a given variable as stochastic may have more to do with generalization and targets of inference than scientific facts. If we wish to generalize to future iterations of a process that will involve a new confounding surface, then we must have a probabilistic model for this new generation.

We caution that conceiving confounding variables as random functions of space in the true data generation process may lead to spurious claims of estimator unbiasedness. That is, in reality, a confounding variable may exist which leads to estimation error (or *conditional* bias), but in imaginary re-generations of the confounding variable, the error would average out to zero (an absence of *unconditional* bias). We contend that the latter fact is mostly irrelevant for scientific purposes. We illustrate this with a toy example in Section 3.1.

Conditional on  $X$ , measured covariates, and  $S$ , we assume that  $Y$  is independent and identically distributed (*iid*). Note that this assumption does not ignore spatial dependence; rather it assumes that any spatial dependence is captured via the function  $U$  of the spatial locations of the observations. This is a typical assumption in many spatial regression models that include flexible functions of space in the regression function and assume that residuals are *iid*.

For simplicity we ignore measured confounders  $C$  in this section but all of the methods discussed below can immediately accommodate measured covariates. We describe several popular spatial models and approaches to spatial confounding, including recent methods developed explicitly for causal inference. We also include methods for inference about  $\beta$ , the coefficient on  $X$  in a regression model of  $Y$  on  $X$ , because such models are often used in practice to derive evidence about the causal effect of  $X$  on  $Y$ , even if the models themselves were originally developed for prediction tasks. We first describe the methods as they are presented in the existing literature, then probe the assumptions under which they succeed in controlling for spatial confounding. Finally, note that some methods described below were developed in the context of areal data (spatial data where “location” refers to a region), though in this manuscript we are most interested in geostatistical data, in which locations are point-referenced.

### 3.1 Ordinary Least Squares

The naive, unadjusted estimate of the effect of  $X$  on  $Y$  is given by the second component of the ordinary least

squares (OLS) estimator

$$\hat{\beta}_{OLS} = (\mathbf{X}'\mathbf{X})^{-1}\mathbf{X}'\mathbf{Y}$$

where the design matrix  $\mathbf{X}$  includes the exposure of interest and intercept, and  $\mathbf{Y}$  is the vector of outcome values. It is well-known that this procedure does not adjust for spatial confounding, but it is the strawman to which spatial confounding proposals are often compared.

Recall the contention above that conceiving of effects as "random" may lead to spurious claims of estimator unbiasedness. For example, any model can be expanded in such a way as to render the unadjusted estimator "unbiased." Consider the following hierarchical model:

$$\begin{aligned} r &\sim \text{unif}(-1, 1) \\ X_i, U_i &\sim_{iid} N(\mathbf{0}, \begin{bmatrix} 1 & r \\ r & 1 \end{bmatrix}) \\ Y_i &\sim_{iid} N(X_i + U_i, 1) \end{aligned}$$

In any given realization of such a data set,  $U$  is a confounding variable and should be included in a regression of  $Y$  on  $X$  to avoid a (conditionally) biased estimate of the true slope. However, in repeated sampling, the average correlation of  $U$  and  $X$  is 0, and thus the unadjusted estimator is (unconditionally) unbiased.

### 3.2 Partially linear models

Many models commonly used to control for spatial confounding fall into the class of *partially linear models* (PLM), which may be written

$$(2) \quad Y_i = \alpha + \beta X_i + g(S_i) + \epsilon_i$$

Here,  $\epsilon_i$  is random error and  $g$  is an unknown, smooth function of space. The outcome is linear in the exposure but nonlinear in spatial coordinates, hence the terminology. It follows from Equation 1 that the estimand  $\beta$  corresponds with the true causal effect of exposure under the assumptions of ignorability and correct specification of the PLM.

Many methods are available to estimate PLMs in spatial contexts. Historically these models were typically used for interpolation [21], but more recently researchers have focused on inference about  $\beta$  (e.g. [36], [50], [22]). While the PLM often connotes a fixed function  $g$ , we note that approaches (described below) such as GP regression can, under suitable conditions, be consistent for the parameter of a PLM [78].

**3.2.1 Splines** Splines, or "smoothing splines," are a family of methods often used to estimate PLMs (equation 2). A spline estimator  $\hat{g}$  of  $g$  is composed of a linear combination of basis functions placed at various locations ("knots") in the domain;  $\hat{g}$  is constructed so as to minimize in-sample error while maximizing smoothness, typically measured by the "wiggliness"  $\int \hat{g}''^2 ds$ . (The order

of the derivative used to measure wiggliness can vary, but in all following formulas below we will assume order 2.)

As with generalized additive models (GAMs) that have been used to adjust environmental data for time trends [19], certain spline models have become popular for adjusting for spatial trends as captured by  $g$ . The model makes no assumption about the relationship between  $g(S)$  and  $X$ , but in general they may be correlated, in which case  $g(S)$  may be interpreted as an unmeasured confounding variable. Consistency of spline estimators in PLM has been established in [56].

Notable for its widespread use is the "thin plate regression spline" (TPRS) [77], a low-rank smoother which solves certain computational issues associated with approximating functions of multidimensional inputs,  $S$  being 2-dimensional for typical spatial applications. Specifically, with a radial basis, the spline optimization problem requires a quadratic optimization involving the similarity matrix  $\mathbf{E}$  where

$$\begin{aligned} E_{ij} &= \frac{1}{8\pi} r_{ij}^2 \log r_{ij} \\ r_{ij} &= \|S_i - S_j\| \end{aligned}$$

which takes  $O(n^3)$  operations, infeasible in large samples. To overcome this, TPRS replaces  $\mathbf{E}$  with a rank- $k$  approximation  $\mathbf{E}_k$ . With the spectral decomposition

$$\mathbf{E} = \mathbf{U}\mathbf{D}\mathbf{U}'$$

arranged so that the diagonal entries of  $\mathbf{D}$  are in descending order of absolute value, we take

$$\mathbf{E}_k = \mathbf{U}_k \mathbf{D}_k \mathbf{U}'_k$$

where  $\mathbf{U}_k$  is the first  $k$  columns of  $\mathbf{U}$  and  $\mathbf{D}_k$  is the diagonalization of the first  $k$  eigenvalues.

**3.2.2 Gaussian process regression** The Gaussian process regression model involves the regression of an outcome variable linearly onto a set of covariates and an additive smooth spatial component  $w(S)$ , i.e.,

$$(3) \quad Y_i = \alpha + \beta X_i + w(S_i) + \epsilon_i; \quad \epsilon_i \sim N(0, \tau^2)$$

The functional form of GP regression is exactly same as the PLM (equation 2). However, the smooth function  $w$  is modeled as a random function and given a Gaussian process (GP) prior. This makes the GP regression model a linear mixed model with a linear covariate fixed effect and a nonlinear spatial random effect modeled as a GP.

A Gaussian process  $\mathbf{w} = \{w_l : l \in \lambda\}$ ,  $\lambda$  being some infinite set, is an infinite collection of random variables such that any finite subset has a multivariate normal distribution. In spatial applications, each variable  $w_l$  is associated with a location so that it can be written  $w_l = w(S_l)$ . This is the point-reference data analog of random effects models for areal data.

For a given domain, the distribution of a Gaussian process is defined by a mean  $\mu(s)$  and covariance function  $K(S_1, S_2)$ . It is common to model Gaussian processes as mean-zero (note that this does not imply that its values in a single realization are centered at zero), isotropic and stationary, which means that  $K(S_i, S_j) = K(|S_i - S_j|)$ ; so a given Gaussian process is determined by a function  $K : \mathbb{R} \rightarrow \mathbb{R}$ .

For estimation in the GP regression model, one can either opt for a fully Bayesian strategy, assigning priors to  $\beta$  and other (covariance) parameters, and proceeding with posterior-based inference. Alternatively, if the errors  $\epsilon_i$  are *iid* Gaussian with variance  $\tau^2$ ; one can marginalize over the spatial random effects  $w$  to obtain the marginal likelihood

$$(4) \quad \mathbf{Y} \sim (\beta \mathbf{X}, \mathbf{K}(\theta) + \tau^2 I)$$

which is then maximized over the parameters  $\beta, \theta$ . Here  $\mathbf{K}(\theta)$  is the matrix whose  $i, j$  entry is  $K(S_i, S_j | \theta)$ .  $\tau^2$  represents residual noise, which may be referred to as the "nugget" or microvariation.

The maximum marginal likelihood estimate of  $\beta$  is given by the generalized least square (GLS) estimate (see Section 3.3).

### 3.3 Generalized least squares

A generalized least squares (GLS) model assumes

$$\mathbf{Y} \sim N(\mathbf{X}\beta, \Sigma(s))$$

where  $\Sigma(s)$  is a covariance matrix, typically such that closer pairs of observations have higher correlations than more distant pairs of observations. The relationship between GP and GLS can be seen by recognizing that GLS groups  $w$  and  $\epsilon$  into one correlated error term. Given  $\Sigma$ , the maximum likelihood estimate for  $\beta$  is

$$\hat{\beta}_{GLS} = (\mathbf{X}'\Sigma^{-1}\mathbf{X})^{-1}\mathbf{X}'\Sigma^{-1}\mathbf{Y}$$

This requires the inversion of the covariance matrix, which can be computationally challenging for large sample sizes.

Note that under the assumption of a multivariate normal distribution for  $\mathbf{Y}$  with mean  $\mathbf{X}\beta$ , the expectations of GLS and OLS estimates are identical. The GLS model is designed to account for dependence in the data, thus improving efficiency and producing valid variance estimators, but does not address bias arising from unmeasured variables. However, GLS estimates coincide with the estimates of marginalized Gaussian process regression (theoretically and in practice depending on implementation, particularly on how the covariance parameter is estimated) described previously in (4), which is a sensible way of controlling for spatial confounding in a partially linear model. To understand this, note that the GLS model assumes that errors are uncorrelated with predictors in the

data generating process, but the estimation procedure may still be used when this assumption is violated. Therefore, it is possible in theory to use GLS point estimates to control for spatial confounding as long as the model is not taken literally.

### 3.4 Restricted spatial regression

In the context of areal data, [36] introduced the restricted spatial regression (RSR) model, a version of which we describe here adapted to point-referenced data where RSR can be conceived of as a GP model where it is assumed that the column space of  $\mathbf{K}(\theta)$  is orthogonal to  $X$ . Beginning with a traditional linear model with random effects

$$(5) \quad \mathbf{Y} = \mathbf{X}\beta + \mathbf{W} + \epsilon$$

with  $\mathbf{W}$  capturing spatial effects through a multivariate normal distribution and  $\epsilon$  being residual noise, we decompose  $\mathbf{W}$  using the projection matrix  $\mathbf{P}_X = \mathbf{X}(\mathbf{X}'\mathbf{X})^{-1}\mathbf{X}'$  and only use the component orthogonal to  $\mathbf{X}$  to give the new model

$$\mathbf{Y} = \mathbf{X}\beta + (\mathbf{I} - \mathbf{P}_X)\mathbf{W} + \epsilon$$

We now have fixed effects and random effects which are completely orthogonal to each other; thus, including the spatial effects does not change the fixed effect estimate and  $\hat{\beta}_{RSR} = \hat{\beta}_{OLS}$ .

The fact that the traditional mixed-effects model does, like the GP regression model or the GLS estimate, change the fixed effect estimate was seen as a problem by [36], who wrote "it seems perverse to use an error term to adjust for the possibility of missing confounders"; hence the motivation for RSR. This overlooks the fact that such methods can be consistent for the parameter of a PLM, as discussed above. On the other hand, the OLS estimate (and hence the RSR estimate) will certainly be biased in the presence of spatial confounding. As we will demonstrate in Section 4, spatial information can be sufficient to adjust for missing confounders, and the formal mathematical device for doing so, whether it be a spline or a Gaussian process prior, is immaterial as long as the researcher has a clear conception of the goals of the analysis and the assumptions required.

The viewpoint of [36] can perhaps be seen as stemming from assuming the mixed-effects model (equation 5) as the data generating process instead of the PLM, in which case we have  $E(\mathbf{Y}) = \mathbf{X}\beta$ . The GLS estimate, accounting for spatial structure via the error term, will always differ from the OLS estimate in finite samples although both are unbiased estimators. The GLS estimate may also have worse finite sample bias than the OLS one especially if the working covariance matrix of  $\mathbf{W}$  is far from the true covariance of  $\mathbf{W}$ . However, if equation (5) is indeed the true data generating process, then the OLS will always

be unbiased and there is no need for any adjustment like RSR. Indeed, assuming (equation 5) as the true data generating process, RSR has been criticized by [40] and [79] on the basis of being “anti-conservative” in the context of the linear mixed model (equation 5), but we emphasize that with respect to the issue of causal confounding, RSR does not even attempt to supply an unbiased effect estimate; rather, it assumes there is no confounding bias.

### 3.5 Spatially-varying coefficient model

A spatially-varying coefficient model [28] maintains the assumption of a linear outcome regression but allows the slope of the regression to vary by location. The model may be written

$$Y_i = \alpha + g(S) + (\beta + h(S))X_i + \epsilon_i$$

where  $g, h$  can either be modeled using spline or Gaussian process and  $\epsilon$  is an *iid* error term. Here,  $g$  controls for confounding and  $h$  allows effect heterogeneity, both of which are assumed to be smooth in space. [28] discuss the specification of a Bayesian model, and [27] evaluate various methods of posterior sampling. [25] propose a profile likelihood approach based on frequentist asymptotics. Recent computational advances in profile likelihood model-fitting can be found in [15]. [49] (see Section 3.8.3) make use of a spatially varying coefficient model with improved robustness.

### 3.6 Two-stage partially linear models

In the spline model, a parameter  $\lambda$  controls the extent of the wigginess penalty. Higher values of  $\lambda$  penalize wigginess more; lower values penalize wigginess less. Under regularity conditions and technical assumptions about the asymptotic regime of the data-generating process, the spline coefficient estimate in the partially linear model has the following properties, assuming  $\lambda \approx n^{-\delta}$  for some  $0 < \delta < 1$  [22]:

$$E[\hat{\beta}] - \beta = o(n^{-1/2}) + O(\lambda^{1/2})$$

$$\text{var } \hat{\beta} = O(n^{-1})$$

In order to construct confidence intervals, it is desirable for the bias to converge at a rate faster than the standard deviation. This would require  $\lambda = o(n^{-1})$ . However, it can be shown that as  $n \rightarrow \infty$ , the optimal value of  $\lambda$ , as measured by average mean squared error of fitted values (AMSE), satisfies  $\lambda = O(n^{-2/3})$ , which does not ensure that the bias converges faster than the standard deviation. This is the problem originally identified by [56]; in order to attain suitable convergence rates for coefficient estimates, the spline fit must be “under-smoothed.”

Two methods, the geoadditive structural equation model (gSEM) [67] and spatial+ [22], are designed to alleviate regularization bias in the partially-linear model via two-stage regression; they take the residuals of a spatial spline

model of the exposure and use them as explanatory variables in a linear regression of the outcome. (They differ in that the latter includes a spline term in the second regression, while the former does not.)

That is, we first fit the model  $X_i = h(S_i) + \delta_i$  and take  $\tilde{X}_i = X_i - \hat{h}(S_i)$ . Then under gSEM, we write  $Y_i = \beta \tilde{X}_i + \epsilon_i$  while for spatial+, we have the model  $Y_i = \beta \tilde{X}_i + g(S_i) + \epsilon_i$ . [67] do not give much mathematical analysis of their method, relying mainly on conceptual and simulation-based arguments. As [22] write, “it is not immediately clear why the method works.” However, [22] give extensive asymptotic results for their own method, spatial+.

Specifically, let  $\lambda_x$  be the penalty parameter of the exposure model and  $\lambda$  be the penalty of the outcome model; assume they satisfy  $\lambda \approx n^{-\delta}, \lambda_x \approx n^{-\delta_x}, 0 < \delta, \delta_x < 1$ . Letting  $\hat{\beta}^+$  denote the new estimator, the following properties hold:

$$E[\hat{\beta}^+] - \beta = o(n^{-1/2}) + O((\lambda \lambda_x)^{1/2})$$

$$\text{var } \hat{\beta}^+ = O(n^{-1})$$

With regularity conditions, however, the AMSE-optimal rates for  $\lambda$  and  $\lambda_x$  are  $O(n^{-2/3})$  and  $O(n^{-2/3}(\log n)^4)$ , respectively. Therefore, with optimal rates, we have  $\lambda \lambda_x = o(n^{-1})$ , and therefore the bias of the estimate converges faster than the standard deviation, and thus no under-smoothing is necessary.

### 3.7 Limitations

With the exception of RSR (and OLS, which yields the same estimate), the methods described above can be used to estimate causal effects under two sets of assumptions: (1) causal identification assumptions that ensure that controlling for a flexible function of space suffices to control for unmeasured spatial confounding (see Section 4 for a rigorous exploration of these assumptions), and (2) correct parametric specification of the spatial regression models used in each of these methods. In terms of parametric assumptions, most of the aforementioned methods (except the SVC model) assume homogeneous effects quantified by the coefficient  $\beta$  in the PLM (equation 2) or the LMM (equation 5). Also, all of the methods described above assume linear exposure effects and an additive spatial effect. These assumptions are extremely strong and likely to be unreasonable for many physical exposures. Common toxicological models often include a *threshold*, or a value below which an exposure has negligible effect [12], which is a clear violation of linearity. Recent work in spatial statistics has recognized the shortcoming of the linearity assumption and have extended the Gaussian process regression equation (3) to allow for nonlinear covariate effects fitted flexibly using random forests or boosting thereby creating GLS versions of these machine learning

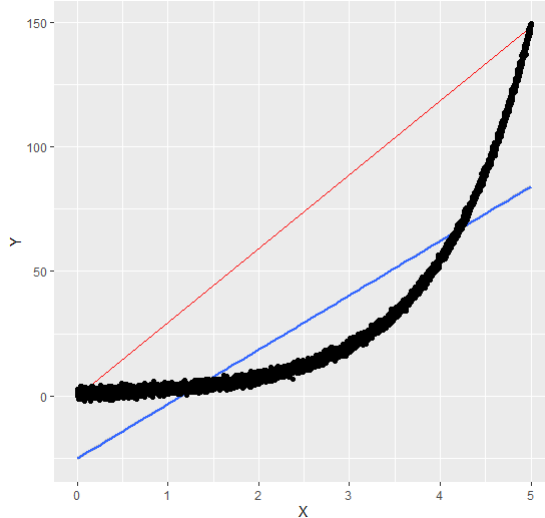


FIG 1. The red line has slope equal to the average incremental effect of intervention on exposure; the blue line is the OLS fit.

procedures [58, 62]. However, these extensions still rely on the additive spatial effect assumption, implying that the effect of exposure is homogeneous in covariates. This may not always be appropriate. For example, air pollution may have more serious effects on older adults and children compared to younger adults, a violation of homogeneity [30].

Intuitively, researchers may believe that departures from model assumptions of linearity and homogeneity “average out” to yield an accurate estimate even in the presence of model misspecification. [1] demonstrates that the average causal effect estimated by a model which (incorrectly) assumes effect homogeneity is an average of the heterogeneous effects weighted by conditional variance of exposure, which may be quite different from the desired uniform average. And if a linear model is used to estimate a nonlinear effect, the resulting estimator need not correspond to a meaningful average, as the following synthetic example demonstrates (see Figure 1).

$$X \sim \text{unif}(0, 5), \quad Y \sim N(\exp(X), 1)$$

In this case, the average effect of incremental intervention (that is, the average slope of the exposure-response curve) on  $X$  may be calculated as

$$E\left[\frac{dE[Y]}{dX}\right] = E[\exp X] = \int_0^5 e^x dx / 5 \approx 29.5$$

But linear regression will approximately minimize  $\int_0^5 (e^x - (\beta_0 + \beta_1 x))^2 dx$ , resulting in an effect estimate of 21.7.

This highlights the need for more flexible nonparametric approaches to spatial confounding, and to causal inference in spatial settings more broadly. We propose one such approach in Section 5.

### 3.8 Recent causal advances

**3.8.1 Distance adjusted propensity score matching** For binary exposures  $X = 0, 1$ , the propensity score  $e(C)$  is defined as the probability of receiving exposure conditional on confounders  $C$ ; or  $e(C) = P(X = 1|C)$ . The importance of propensity scores derives from their “balancing property”: if exposure is unconfounded conditional on  $C$ , then exposure is unconfounded conditional on  $e(C)$ . This suggests the procedure of propensity score matching, in which propensity scores are estimated for all individuals, and then treated individuals are matched with untreated individuals with the nearest propensity score. This sample of matched individuals mimics a pseudo-population in which exposure is unconfounded; thus, the effect of exposure in this pseudo-population can be estimated from the observed data. The pseudo-population typically differs from the original population in that it excludes individuals with extreme propensity scores (i.e., those close to zero or one). A review of the use of propensity score matching for confounding adjustment can be found in [64].

The traditional propensity score matching procedure is insufficient to control for unmeasured confounding. However, [51] adjust the procedure in a way that may, under causal assumptions like those in Section 4 below, mitigate unmeasured spatial confounding. They introduce a dissimilarity measure  $d_{ij}$  where

$$d_{ij} = w * |e(C_i) - e(C_j)| + |S_i - S_j|$$

Thus  $d_{ij}$  incorporates relevant differences in observed confounders (as captured through the propensity score) and unobserved confounders (as captured through spatial location), with the weight  $w$  determining the relative importance of the two factors. Matching can then proceed based on  $d_{ij}$  rather than differences in propensity score alone, which ensures matched individuals are similar based on observed and unobserved confounders.

The advertised strength of this method is that it allows the user to adjust (via  $w$ ) the relative importance of measured and unmeasured confounders. However, in doing so, the model makes a restrictive assumption about the form of the propensity score, and it is not clear how reliable an *a priori* guess at  $w$  could be. On the other hand, if one decides to estimate  $w$  from data, it is unclear why this method should be preferred to simply including spatial coordinates in a propensity score model, unless  $w$  itself is of substantive interest.

**3.8.2 CAR model for areal confounding** The conditionally autoregressive model, originating in [6], is a computationally convenient correlation model for areal data that encodes the similarity of neighboring areas. If a variable  $Z$  has a mean-zero CAR structure, then

$$Z \sim N(0, \tau^{-1}(\mathbf{D} - \phi\mathbf{W})^{-1})$$

Here,  $\mathbf{D}$  is a diagonal matrix whose entries are the number of neighbors of the corresponding area, and  $\mathbf{W}$  is the adjacency matrix of areas.  $\tau$  and  $\phi$  are free parameters.

[61] consider the model

$$Y_i = \eta(X_i, C_i) + g(U_i) + \epsilon_i$$

where  $C$  are measured confounders and  $U$  are unmeasured confounders. They proceed by letting  $g(\mathbf{U}) := \mathbf{U}'$  and assuming  $(\mathbf{U}', \mathbf{X})$  has a (joint) CAR structure, thus giving a likelihood model for unmeasured confounding. This differs from a traditional CAR model which only puts the multivariate normal distribution on the random effects, modeling them as independent of the exposure. The paper also considers the estimation of nonlinear effects. However, the method relies on strong parametric identifying assumptions about the relationship between  $\mathbf{U}'$  and  $\mathbf{X}$  and it is not clear when these would hold in practice or how practitioners would reason clearly about them, especially in settings where  $U$  may be an unidentified latent confounder.

*3.8.3 Orthogonalized regression for heterogeneous effects* [49] consider the model

$$Y_i = \beta(S) * X_i + g(S) + \epsilon_i$$

This is equivalent to the spatially-varying coefficient model of Section 3.5, reparametrized for convenience. Taking the residualized versions of the exposure and outcome,

$$W_i := Y_i - E[Y_i|S_i]$$

$$V_i := X_i - E[X_i|S_i]$$

we have the equation

$$W_i = \beta(S_i)V_i + \epsilon_i$$

which eliminates the nuisance function  $g$  from the estimation. The authors describe a novel method for estimating the function  $\beta$  via cubic spline regression in a manner robust to the finite-sample error of the estimates of  $E[Y|S]$  and  $E[X|S]$ . This methodology shares similarities with the spatial+ method of [22] (Section 3.6) but has the advantage of handling heterogeneous effects. However, the methodology deals only with linear exposure effects and has not been explored for curve-fitting methods other than splines.

#### 4. IDENTIFICATION AND ESTIMABILITY IN THE PRESENCE OF SPATIAL CONFOUNDING

In this section we establish conditions for nonparametric identification of causal effects under spatial confounding using the relevant causal definitions overviewed in Section 2.1. We assume consistency (A1) throughout and, without loss of generality, we omit measured covariates

*C*. We assume the existence of a spatially varying confounder  $U$  such that, had  $U$  been observed, causal effects of  $X$  on  $Y$  would be identified. That is, we assume that ignorability and positivity hold conditional on  $U$ :

$$\text{A4. } Y(x) \perp X|U$$

and

$$\text{A5. If } x \in \text{supp}(X) \text{ and } u \in \text{supp}(U), \text{ then } (x, u) \in \text{supp}(X, U)$$

The question we answer in this section is: *Are there assumptions under which causal effects may be estimated using spatial models even if  $U$  is unobserved?* In particular, we will present conditions under which spatial location  $S$  may be used as a proxy for  $U$ . This is the approach taken by all of the methods for spatial confounding considered in the literature – they can be seen as controlling for  $S$  in lieu of  $U$ . But as we will see, the validity of this approach depends on strong and subtle assumptions. We present one set of sufficient (nonparametric) identification assumptions; other alternatives exist, e.g. the parametric approach of [61] for the setting of area-level spatial data, but generally require different analytic methods.

#### 4.1 Ignorability and spatial confounding

Consider draws from a joint distribution  $\mathcal{P}$  defined over variables  $(S, X, Y(x))$ , where  $S$  is spatial location,  $X$  is some exposure, and  $Y(x)$  are potential outcomes. Throughout we make the crucial and strong assumption that the unmeasured confounder  $U$  is spatially varying such that  $U = g(S)$ , where  $g$  is a (possibly unknown) measurable function:

$$\text{A6. } U = g(S) \text{ for a fixed, measurable function } g.$$

Note that  $U$  may not be unique; that is there may be multiple different random variables that each suffice to control for confounding. Technically, it needs only to be the case that Assumption A6 holds for some  $U$  that satisfies Assumption A4.

There are two ways in which an arbitrary unmeasured confounder could fail to be equal to  $g(S)$  for some measurable function  $g$ . First,  $U$  may not be a function of space alone; this is the case whenever two individuals may share a location without sharing a value of  $U$ . For example, if  $U$  is personal income but location is measured at the household level, then  $U$  is not a function of  $S$  alone—though it may depend partially on  $S$ —because members of the same household may have different values for personal income.

On the other hand, even if it can be claimed that  $U$  is a function of  $S$ , it is not necessarily a *measurable* function of  $S$ . On a continuous domain, a measurable function can be thought of as a “nearly continuous” function,

or a continuous function with at most a small set of discontinuities (see “Lusin’s theorem” in [54]). Then even a variable such as household income (as opposed to personal income) does not satisfy this criterion, because the map from spatial location to household income is likely very discontinuous, as there is non-spatial variation in the incomes of neighboring households.

In the case that  $U$  is a measurable function of space plus some residual variation, as might be assumed for a variable like household income, confounding bias may be reduced but its elimination is in general impossible. In other words, including spatial information in a causal analysis could reduce bias compared to omitting spatial information, but causal estimates would still not be consistent. In this setting, the flexible function of  $S$  included in spatial regression models could operate like a surrogate or proxy confounder or a confounder measured with error, but it could not capture the confounder without error. In general, the literature on spatial confounding does not explicitly claim that spatial regression models can eliminate confounding bias; rather the ubiquitous implicit assumption seems to be that a flexible function of  $S$  can mitigate bias due to unmeasured spatially varying confounding. But, tempting though it may be to reason that controlling for a mismeasured confounder or a confounder proxy will always mitigate confounding bias, the reality is considerably more complicated [47, 48, 41, 42, 66, 52]. Following [47, 48], we conjecture that using a flexible function of  $S$  to control for an unmeasured spatially varying confounder will tend to mitigate confounding bias whenever the relationship between  $S$  and  $U$  does not vary with exposure (that is, measurement error is non-differential) and there is no qualitative interaction between the unmeasured confounder and the exposure, but future work is needed to prove or further explore this conjecture.

The following proposition characterizes when conditioning on location  $S$  in lieu of an unmeasured spatial confounder  $U$  suffices for ignorability to hold (possibly also conditional on measured covariates  $C$ , omitted for conciseness). First, we make the assumption that conditioning on  $S$  in addition to  $U$  does not *induce* confounding:

$$A7. \quad Y(x) \perp X|S, U$$

Now we can state the proposition:

**PROPOSITION 1.** *Assumptions A6 and A7 imply  $Y(x) \perp X|S$ .*

**PROOF.** Since  $U = g(S)$  is a measurable function of  $S$ , the double  $(S, U)$  is a measurable function of  $S$  as well. Since  $S$  is trivially a function of  $(S, U)$ , there exists a measurable one-to-one mapping between  $S$  and  $(S, U)$ ;

therefore  $S$  and  $(S, U)$  give rise to the same conditional distributions (formally, they generate the same sigma-algebra). Therefore if  $Y(x) \perp X|(S, U)$ , it also holds that  $Y(x) \perp X|S$ .  $\square$

Assumption A7 is similar to conditional ignorability A4. If the latter is true, the former is often a reasonable assumption; it would typically hold whenever spatial location is causally precedent to exposure and outcome but would be violated if spatial location were a collider between exposure and outcome (i.e., it is influenced by both exposure and outcome) or a descendant of (i.e., influenced directly or indirectly by) such a collider. The assumption is likely uncontroversial in many applications, though this could be complicated in longitudinal studies, especially if there is movement of subjects. (See [24] for a discussion of collider bias.) Assumption A7 may be circumvented in favor of the substantively stronger but possibly more intuitive assumption

$$A8. \quad (Y(x), X) \perp S|U$$

This assumption implies that spatial location only affects the joint distribution of potential outcomes and exposure through the unmeasured confounder. This assumption is reasonable if  $U$  is the only (unmeasured) spatial variable affecting  $X$  or  $Y$ . Together with A4 and A6, this is sufficient for the conclusion of Proposition 1.

## 4.2 Positivity and spatial confounding

A few sources [73, 53, 17] have devoted themselves to discussing the details of the positivity assumption (not in the context of spatial confounding), though it receives considerably less attention in the literature than ignorability. In the context of spatial confounding, [50] and [61] associated the positivity assumption with the assertion that the exposure varies at a smaller scale than the spatial confounder, a point which is also explored in [37], but a rigorous treatment of spatial-statistical concepts and the positivity assumption in causal inference is lacking.

As discussed in Section 2, with outcome  $Y$ , exposure  $X$ , and a measured confounder  $C$ , the positivity assumption is needed to ensure that the conditioning event has positive probability in the expression  $E[E[Y(x)|C, X = x]]$ . If there exists  $x \in \text{supp}(X)$  such that  $c \in \text{supp}(C)$  and  $(x, c) \notin \text{supp}(X, C)$ , then the above functional is not well-defined. If positivity fails, then parametric assumptions such as effect linearity or homogeneity are needed to estimate causal effects. These assumptions can be used to extrapolate from regions of the data where positivity holds to regions where it does not hold. We caution that any conclusions drawn from regions of the data where positivity does not hold are not informed by the data; they are determined entirely by the assumptions used to extrapolate.

In the case of spatial confounding, positivity must hold with respect to  $S$  in order for inference using  $S$  as a proxy for  $U$  to avoid extrapolation. In some settings it may be feasible to reason about this directly, i.e. to assume

A9. If  $x \in \text{supp}(X)$  and  $S \in \text{supp}(S)$ , then  $(x, s) \in \text{supp}(X, S)$ .

Alternatively, if researchers do not have enough *a priori* information about the joint distribution of exposure and spatial location to assess whether Assumption A9 is reasonable, positivity with respect to  $S$  is also guaranteed by the following assumption in conjunction with A5:

A10.  $X \perp S|U$ ; that is,  $S$  is only associated with  $X$  through  $U$ .

The following proposition says that if positivity holds conditional on  $U$ , and  $S$  is only associated with  $X$  through  $U$ , then positivity also holds conditional on  $S$ :

**PROPOSITION 2.** *Assume A5 and A10. Then positivity holds conditional on  $S$ , meaning if  $x \in \text{supp}(X)$  and  $s \in \text{supp}(S)$ , then  $(x, s) \in \text{supp}(X, S)$ .*

**PROOF.** By the former assumption, we have  $pr(X = x|U) > 0$  for each  $x$ . Then, by the latter assumption,  $pr(X = x|U, S) > 0$ . Since  $(U, S) = (g(S), S)$  is a one-to-one function of  $S$ , conditioning on  $(U, S)$  is equivalent to conditioning on  $S$ . Therefore,  $pr(X = x|S) > 0$ .  $\square$

Note that A10 is implied by A8.

In practice, the relevant consideration regarding positivity conditional on spatial location is whether there is a sufficient mix of exposure levels within reasonably small regions of the confounder space. A sufficient condition for this discussed in [50] is the existence of a finer spatial scale of variation for  $X$  compared to  $U$ ; if  $X$  varies faster than  $U$ , then areas with similar values of  $U$  will exhibit wide ranges of values of  $X$ . For continuous confounders, these interpretations are crucial because the probability associated with any particular confounder value is zero. Note that under the assumption that  $U$  is a measurable function of  $S$ , then small neighborhoods of  $S$  will typically contain small regions of the confounder space  $U$ , hence the connection between the two conditions, though we note that a quickly varying function may still be measurable or even continuous (for example, a sinusoidal function with small period) in which case, exposure would need to vary at even higher scale for positivity to hold. Given that in most scientific applications there will be non-infinitesimal space between observations, it may be difficult to differentiate even in principle between a quickly varying smooth function and a non-measurable function, but a thorough discussion of this subtlety is beyond the scope of this paper.

### 4.3 Estimability

Under assumptions A5, A7, and A10; or A4, A5, and A8; or A7 and A9 (and, in any event assuming A6); causal effects are nonparametrically identified using  $S$  instead of  $U$ : following the logic of Section 2.1,  $E[Y(x)] = E[E[Y|X = x, S]]$ . This suggests that the same estimation strategies that would be used to control for  $U$  if it were observed may also be applied using  $S$ . Indeed, this seems to be the strategy behind most of the methods reviewed in Section 3. In this section we present sufficient conditions under which this is indeed the case, but caution that it may not be in general.

First, it must be the case that  $g(S)$  is regular enough, in some sense, to be estimable by the chosen strategy. No method can well-approximate an arbitrarily complex function in finite samples, therefore all of the methods discussed above and described below make some assumptions about the complexity of  $g(S)$ . For example, spline methods assume that the function is smooth.

Second, it must be the case that the functional form of  $E[Y|X = x, S]$  is compatible with the regression surface that matters for confounding,  $E[Y|X = x, g(S)]$ . Suppose  $E[Y|X, U]$  is linear in  $U$  but  $U$  is a polynomial function of  $S$ . Then a linear regression of  $Y$  onto  $X$  and  $S$  would be misspecified but a polynomial regression would be correctly specified. A challenge in the spatial confounding scenario is that the relationship between  $U$  and  $S$  will generally be an unknown transformation, therefore it may be easier for researchers to reason about modeling assumptions on the basis of  $U$  rather than  $S$ . This points to the need for flexible nonparametric estimation strategies that have a better chance of capturing the true confounding surface in terms of  $S$ .

Conversely, researchers who reason about the functional form of  $E[Y|X, S]$  may miss important interaction or other terms needed to capture  $E[Y|X, g(S)]$ . Suppose the unmeasured confounder  $U$  interacts with  $X$  in its effect on  $Y$ . Then additive models for  $E[Y|X, S]$  that does not include interactions between  $X$  and functions of  $S$  cannot hope to control for confounding by  $U$ . Again, this highlights the need for flexible nonparametric estimation strategies.

### 4.4 Shift interventions

So far we have focused on the nonparametric identification of  $E[Y(x)]$  – but typically the goal of causal inference is to estimate a causal effect rather than a mean potential outcome. In the simplest case, a binary exposure  $X = 0, 1$  admits the notion of an “average treatment effect,” defined as  $E[Y(1) - Y(0)]$ . When  $X$  is continuous, as is often the case with environmental exposures, there is no longer just one quantity which completely specifies the average effect of interventions on  $X$ . One might choose to estimate the entire *exposure-response curve*  $E(Y(x))$  for

all values  $x$ , but it can be convenient to have a more compact characterization of the effect on of interventions on  $X$ . As described in Sec 3, this is typically accomplished by assuming linear and homogeneous treatment effects so that any contrast  $E[Y(x) - Y(x')]$  is a simple function of  $\beta$  from a spatial regression model. However, as we described in Section 3.7, when the operative parametric assumptions do not hold this approach does not necessarily result in interpretable causal effects. While estimation of the exposure-response curve has been explored with robust causal methods of the kind we advocate (e.g. [39]), this kind of functional estimation may be difficult and unnecessary if a low-dimensional effect summary is desired. We will provide an alternative approach.

We define a “shift intervention” as a special case of the class of interventions considered in [33]. A shift intervention is an intervention that assigns to individual  $i$  with exposure  $X_i$  the new exposure  $X_i + \delta$  for some constant  $\delta$ . Thus the expected effect of the shift intervention on individual  $i$  is  $E[Y_i(X_i + \delta) - Y_i(X_i)]$ ; notably, this quantity depends on  $X_i$ . If we are interested in population-level effects, we may define  $\Delta = E[Y(X + \delta) - Y(X)]$ , simply taking the population average of individual effects, where the expectation is taken over the observed data distribution of  $X$ . In other words, the effect of the intervention may depend on what values of exposure are already present in the population. For example, in a threshold model, shift interventions in the positive direction might have no effect if current population levels are far below the threshold, but high effects if current population levels are near the threshold.

As noted above, targeting the shift estimand may be beneficial since it avoids estimating entire functions (like the exposure-response curve), which is challenging with limited data. Aside from feasibility, the shift estimand is advantageous in that it avoids parametric assumptions and relaxes the requirement of positivity. The shift estimand is also easily interpretable and of direct policy relevance in many applications.

Specifically, we can replace the positivity assumption A5 or A9 with the following weaker assumption:

$$A11. \quad (x, c) \in \text{supp}(X, C) \implies (x + \delta, c) \in \text{supp}(X, C)$$

Recall that (standard) positivity would entail that each level of confounder values corresponds to a positive probability of receiving *any* exposure. This assumption, which we may call “shift positivity”, on the other hand, is satisfied if every confounder value has positive probability of exposure values within  $\delta$  of its observed exposure value. In the case of spatial confounding, if A11 holds for  $C = U$ , and A10 is satisfied, then A11 also holds for  $C = S$ ; the logic is identical to that of the case of positivity. Shift positivity may be a more reasonable assumption for exposures such as air pollution, where there may

be variation over relatively small regions, but not enough variation to cover the entire range of exposure values seen across large regions.

Targeting the shift estimand does not require the assumption of a linear or homogeneous model since it represents the *average* expected change over all subjects if all their exposures were shifted by a certain amount, regardless of whether each subject would be expected to display the same change in outcome. The shift estimand is therefore a way of summarizing causal processes down to one scalar quantity even if the causal process is heterogeneous or nonlinear. (If the shift is infinitesimal, then this corresponds to the discussion of Figure 1.) Note that when the true data-generating process is linear in  $X$  (i.e.,  $E[Y|C, X]$  is a linear function of  $X$ ), the shift intervention estimand for a unit shift coincides with the ordinary linear coefficient, but the coefficient in a linear model signifies the expected change in *every* subject’s outcome that would be brought by a one-unit increase in exposure; for this to be meaningful both linearity and homogeneity must be satisfied.

With this in mind, it is easy to see why the shift estimand is of direct policy relevance: it is more practical to consider interventions that incrementally change each individual’s exposure by some amount (for example, what would be the average effect on life-expectancy if PM<sub>2.5</sub> levels were decreased everywhere by  $2\mu\text{g}/\text{m}^3$ ), rather than adjusting all individuals’ exposure levels to some common new level which may be far from their current values (which is the intervention directly considered by estimation of the exposure-response curve). Finally, by summarizing complex data generating processes down to a single quantity, the shift estimand is valuable for its interpretability.

## 5. FLEXIBLE MODELS FOR SPATIAL CONFOUNDING

In this section we assume that the identifying assumptions from Section 4 hold, that is that the causal effect of  $X$  on  $Y$  is nonparametrically identified using  $S$  as a proxy to control for unmeasured confounding by  $U$ . We now turn to estimation strategies and discuss semi- and nonparametric alternatives to the spatial regression models from Section 3. Our key insight is that controlling for  $S$  is fundamentally no different from controlling for any other measured confounder, and there is no need to restrict estimation methods to traditional spatial regression models. First we present a general nonparametric spatial regression model, but our focus is on *doubly robust* methods that model both the outcome conditional on  $X$  and  $S$ , as in the spatial regression methods, and the exposure conditional on  $S$ , i.e. the propensity scores. This methodology has been employed in causal inference for decades (see [5] for a relevant exposition) but has not, to our knowledge, been employed in spatial statistics. A doubly robust

estimator consistently estimates the causal effect of interest if either one of the two models is correctly specified; typically doubly robust estimators are efficient when both are correctly specified. In the case where the outcome and exposure models are both nonparametric, this estimation strategy is referred to as DML. It can be shown that in such models, the asymptotic error of the DML model behaves as a product of the asymptotic errors of the two component models, thus increasing efficiency, improving rates of convergence, and allowing causal effects to be estimated at parametric  $n^{1/2}$  rates even when the postulated models only converge at rate  $n^{1/4}$  [9].

In general, it is preferable not to impose strong assumptions on the data-generating process, but it is especially important in the context of spatial confounding. This is because any scientific knowledge that could justify restrictive assumptions would likely come from understanding of the process involving the physical unmeasured confounder variable rather than spatial location itself. A more flexible class of regression models than the ones discussed in section 3 may be written as

$$Y_i = f(X, S) + \epsilon_i$$

where  $S$  is typically two-dimensional and the error terms  $\epsilon$  have expectation zero and are independent of confounders, exposure, and each other.

Numerous algorithms may be used to estimate the regression function  $f$ . We will compare multidimensional spline smooths (in the `mgcv` R package) on the joint space of  $X$  and  $S$ , multidimensional Gaussian processes (in the `kernp` R package) on the joint space of  $X$  and  $S$ , random forests (in the `randomForest` R package), and BART (Bayesian additive regression tree, in the `dbarts` R package). The spline and Gaussian processes only rely on the assumption that the regression function is smooth in its inputs. Tree-based models (random forest and BART) do not make the assumption of a smooth function; rather, they approximate arbitrary functions by estimators that are piecewise constant over rectangles in the input space [7, 10].

Under the identification assumptions, these regression techniques are sufficient to estimate causal parameters including the exposure-response curve. However, as mentioned above, it may be difficult and unnecessary to estimate the entire exposure-response curve. In addition, using machine learning outcome regression alone (as opposed to in a DML framework) to estimate causal parameters with complex confounding can lead to extremely unreliable confidence intervals [46]. Estimating a shift estimand using doubly-robust methods can give more reliable and interpretable results for causal estimands with complex spatial confounding.

## 5.1 Doubly robust estimation

We now turn to doubly robust estimation, first with parametric outcome and propensity score models and then with DML. Doubly robust versions of the nonparametric outcome regression (equation 5) are available, e.g. [39], but following the discussion in Section 4.4 we instead focus here on methods originally proposed by [33] for doubly robust estimation of a shift intervention.

The following provides a discussion of a specific case of the methodology presented in [33] to estimate the shift interventions discussed in Section 4.4.

For  $\mu_\delta := E[Y(X + \delta)]$  and  $E[Y(X)] = \mu_0$ , the estimand of interest is  $\Delta = \mu_\delta - \mu_0$ . The latter term can clearly be estimated by the empirical outcome mean  $\hat{\mu} = \bar{y}$ , so we will focus on the estimation of the former quantity.

Under our assumptions,  $\mu_\delta$  is identified by  $E[E[Y|X + \delta, C]]$ , suggesting that  $n^{-1} \sum_{i=1}^n \hat{f}(X_i + \delta, S_i) := \hat{\mu}_{\delta, R}$  will be a consistent estimator of  $\mu_\delta$  as long as  $\hat{f}(X_i + \delta, S_i)$  is consistent for  $f(X, S) = E[Y|X, S]$ . This is the outcome regression estimator.

On the other hand, we also have the identity

$$\mu_\delta = E[\lambda(X, S)Y]$$

where

$$\lambda(X, S) = \frac{p(X - \delta|S)}{p(X|S)}$$

with  $p$  a probability density, because

$$\begin{aligned} & E\lambda(X, S)Y \\ &= \int \int \int \frac{p(X - \delta|S)}{p(X|S)} Y p(S)p(X|S)p(Y|X, S)dSdXdY \\ &= \int \int \int p(X - \delta, S)Y p(Y|X, S)dSdXdY. \end{aligned}$$

This is the conditional expectation of  $Y$  when  $X$  is shifted by  $\delta$ , and so ignorability yields that the expression above is equal to  $E[Y(X + \delta)] = \mu_\delta$ .

Thus it is possible to estimate the potential-outcome shifted mean either by modeling the outcome process or the exposure process. In the following way, these two strategies may be combined.

Let  $\hat{f}$  be an estimator of  $E[Y|X, S]$  and  $\hat{\tau}$  be an estimator of  $p(X|S)$ . We solve the following estimating equation for  $\gamma$ :

$$\sum_{i=1}^n \hat{\lambda}(X_i, S_i)(Y_i - \hat{f}(X_i, S_i) - \gamma \hat{\lambda}(X_i, S_i)) = 0$$

where  $\hat{\lambda}$  means an estimate of  $\lambda$  based on  $\hat{\tau}$ . As a parametric strategy, this equation may be solved by fitting a

linear model for  $Y$  with the covariate  $\hat{\lambda}(X_i, S_i)$ , no intercept, and the offset  $f(X_i, S_i)$ . Then the doubly robust estimate of  $\mu_\delta$  is given by

$$\hat{\mu}_{\delta, DR} = n^{-1} \sum_{i=1}^n (\hat{f}(X_i + \delta, S_i) + \hat{\gamma} \hat{\lambda}(X_i + \delta, S_i))$$

The details of the convergence of  $\hat{\mu}_{\delta, DR}$  can be found in the appendix of [33]. To see the double-robustness, first assume the exposure model is consistent, without any assumption on the outcome regression. Note that for any function  $h$ , we have  $E[\lambda(X, S)h(X, S)] = E[h(X + \delta, S)]$ . Therefore, in large samples, the solution of the estimating equation will converge to the solution of the equation

$$\sum_{i=1}^n \lambda(X_i, S_i) Y_i = \sum_{i=1}^n \hat{f}(X_i + \delta, S_i) + \gamma \lambda(X_i + \delta, S_i)$$

Since  $E[\lambda(X_i, S_i)Y_i] = \mu_\delta$ , we can divide the above equation by  $n$  to see that the law of large numbers implies that  $\hat{\mu}_{\delta, DR} \rightarrow \mu_\delta$  as well.

On the other hand, if the outcome regression is consistent, then in large samples, the solution of the estimating equation will converge to the solution of the equation

$$\begin{aligned} \sum_{i=1}^n \hat{\lambda}(X_i, S_i) (Y_i - E[Y_i|X_i, S_i] - \gamma \hat{\lambda}(X_i, S_i)) &= 0 \\ \sum_{i=1}^n \hat{\lambda}(X_i, S_i) (Y_i - E[Y_i|X_i, S_i]) - \gamma \hat{\lambda}^2(X_i, S_i) &= 0 \\ \implies \gamma &\rightarrow \frac{\sum_{i=1}^n \hat{\lambda}(X_i, S_i) (Y_i - E[Y_i|X_i, S_i])}{\sum_{i=1}^n \hat{\lambda}^2(X_i, S_i)} \\ &= \frac{n^{-1} \sum_{i=1}^n \hat{\lambda}(X_i, S_i) (Y_i - E[Y_i|X_i, S_i])}{n^{-1} \sum_{i=1}^n \hat{\lambda}^2(X_i, S_i)} \\ &\rightarrow \frac{E[\hat{\lambda}(X_i, S_i) (Y_i - E[Y_i|X_i, S_i])]}{E[\hat{\lambda}^2(X_i, S_i)]} \end{aligned}$$

Note that  $Y - E[Y|X, S]$  is uncorrelated with any function of  $(X, S)$ . Therefore, as long as  $\hat{\lambda}$  converges some function other than the constant 0, we have  $\gamma \rightarrow 0$ . Thus  $\hat{\mu}_{\delta, DR}$  will asymptotically be based (to the first order) only on  $\hat{f}$  and hence consistent. When the outcome regression and exposure models are both consistent  $\hat{\mu}_{\delta, DR}$  asymptotically achieves the semiparametric efficiency bound, as noted by [38].

**5.1.1 Double machine learning** Among consistent estimators of an estimand of interest, it is generally preferable to choose one with a fast rate of convergence; in particular, convergence at the rate of  $n^{-1/2}$  is desirable for standard asymptotic results and the construction of confidence intervals. When estimating causal effects in

the presence of complex or high-dimensional confounding, flexible “machine learning” methods may be beneficial relative to more restrictive methods which risk model misspecification. However, the flexibility of these methods often come at the cost of slower rates of convergence. To combat this difficulty, a strategy similar to doubly robust estimation may be employed via sample-splitting and “orthogonalized” estimation, as laid out in [9]. A kernel smoothing estimator proposed by [39] specialized this procedure for continuous exposures; the work of [38] offers some general results for interventions that incrementally shift propensity scores.

When machine learning methods are employed to estimate both the outcome and exposure models using the doubly robust procedure described above, the causal effect estimate converges as quickly as the product of the rates of convergence of those two models, yielding a  $n^{-1/2}$  convergence rate as long as the models attain the relatively slow rate of  $n^{-1/4}$ .

Spatial confounding is not necessarily high-dimensional in the sense of involving a high number of adjustment variables, but the complexity of nuisance functions can be expected to be considerable, since any unmeasured confounder may be a complicated function of spatial location, even if that function is smooth. Therefore, the DML is a strong candidate for controlling for spatial confounding.

## 6. SIMULATIONS

The purposes of the following simulations are to show the limitations of parametrically restrictive models when their assumptions do not hold, and to compare existing popular estimators with modern causal methods, in particular DML. In addition, we simulate scenarios where no methods are capable of returning consistent results due to noise in the confounding surface or smoothness of the exposure. We investigate data generating processes involving an unmeasured spatial confounder that influences both exposure and outcome. In each case, the exposure is continuous; the causal contrast of interest is the effect of an intervention shifting the exposure by +1. The locations are generated uniformly at random on the  $[-1, 1] \times [-1, 1]$  square, and new locations are drawn in every replicate. In the small-sample simulations, 1000 observations are generated for 500 replicates. In the large-sample simulations, 10,000 observations are simulated for 250 replicates. By design, the true effect in all simulations except the nonlinear effect scenario is 1. In the nonlinear effect scenario, the true effect was assessed by simulation to be 2.431.

### 6.1 Estimators

The methods under consideration are listed below. Algorithms implemented in external packages are run with default settings. (Due to computational constraints,

not every method is used in the large-sample simulations.) Confidence intervals are for 95% nominal coverage. Bootstrap confidence intervals use 120 resamples to obtain a normal approximation to the sampling distribution, as recommended in [23].

For linear models, we use the linear coefficient estimate to estimate the effect of a +1 shift intervention. For other models, other than the DML methods, we use the model to predict potential outcomes under the shift intervention and then take the average difference with the models fitted observed values. For the DML methods, we use the procedure of [34] described above.

- RSR [36] (unadjusted estimator). Confidence intervals by bootstrap.
- spline: PLM with spatial effect modeled by thin plate regression spline [77]. Implemented by `mgcv` [76]. Analytic confidence intervals.
- gp: PLM with spatial effect modeled by two-dimensional nearest-neighbors Gaussian process (NNGP) [59]. Implemented by `BRISC` package [60]. Confidence intervals by `BRISC` bootstrap.
- gSEM: geo-additive structural equation model [67]. Splines fit by `mgcv`. Confidence intervals by bootstrap.
- spatial+: spatial+ [22]. Splines fit by `mgcv`. Confidence intervals by bootstrap.
- svc\_mle: Spatially-varying coefficient model [15]. Implemented by `varycoef` package [16]. Confidence intervals omitted (since resampled points cannot be accommodated by the GP covariance function).
- spline\_interaction: Spline with spatial interaction of exposure and space (hence, a spatially-varying coefficient model). Implemented by `mgcv`. Confidence intervals by bootstrap.
- gp3: Three-dimensional Gaussian process over location and exposure (flexible model). Implemented by `RobustGaSP` [31]. Confidence intervals omitted (since resampled points cannot be accommodated by the GP covariance function).
- spline3: Three-dimensional spline over location and exposure (flexible model). Implemented by `mgcv`. Confidence intervals omitted due to computational constraints.
- rf: Random forest over location and exposure (flexible model) [7]. Implemented by `randomForest` package [45]. Confidence intervals by bootstrap.
- BART: Bayesian additive regression tree (BART) over location and exposure (flexible model) [10]. Implemented by `dbarts` [20] package. Confidence intervals by bootstrap.
- DML\_gp3: gp3 model augmented with spline model over space for exposure (flexible model, DML). Confidence intervals omitted (since resampled points

cannot be accommodated by the GP covariance function).

- DML\_spline: spline3 model augmented with spline model over space for exposure (flexible model, DML). Confidence intervals omitted due to computational constraints.
- DML\_BART: BART model augmented with spline model over space for exposure (flexible model, DML). Confidence intervals by bootstrap.

## 6.2 Notes on implementation

We use package-default settings in general, but we adjust the parameter  $k$  in the `mgcv` package which controls the maximum number of degrees of freedom in the spline fits so that they can adequately approximate complicated functions. For splines over two dimensions, we use  $k = 200$ . For three-dimensional splines, we use  $k = 1000$  in the large sample and  $k = 500$  in the small sample.

To estimate the effect of the shift intervention by DML, we implement the procedure described in section 5.1. We fit the exposure model with a thin plate regression spline as  $X_i = g(S_i) + \epsilon_i$  where the errors are *iid*. The *iid* assumption simplifies the estimation of the function  $\lambda$  (by reducing the conditional density estimation to an unconditional density estimation), but the assumption is violated in the heterogeneous effect simulations (in which case errors are independent but not identically distributed). We introduce heteroskedasticity in these scenarios to demonstrate the potential for bias arising from incorrect assumptions of homogeneity. (Under homoskedasticity, this bias can be zero; see [1] which demonstrates that the homogeneous estimate is an average of the population of effects weighted by conditional variance of exposure. Under homoskedasticity, this is equivalent to the unweighted average.)

## 6.3 Simulation settings and results

We consider the following data-generating processes.

### 6.3.1 Linear confounding

$$\begin{aligned} S^a, S^b &\sim_{iid} \text{unif}(-1, 1) \\ U &= S^a + S^b \\ X &\sim N(U, 5) \\ Y &\sim N(3U + X, 1) \end{aligned}$$

The linear confounding scenario, Table 1, is a baseline scenario where there is no complicated spatial confounding; the spatial coordinates enter the data generating process linearly. Therefore, all models except for RSR are correctly specified, and regularization bias for spline models is not a concern (since oversmoothing is not possible). All models that adjust for confounding perform well and have high confidence interval coverage except

n	method	bias	sd	mse	coverage
1000	RSR	$7.733 \times 10^{-2}$	$1.603 \times 10^{-2}$	$6.237 \times 10^{-3}$	0%
1000	spline	$-9.958 \times 10^{-5}$	$6.297 \times 10^{-3}$	<b><math>3.958 \times 10^{-5}</math></b>	96%
1000	gp	$7.932 \times 10^{-4}$	$6.509 \times 10^{-3}$	$4.292 \times 10^{-5}$	95%
1000	gSEM	$1.362 \times 10^{-3}$	$7.017 \times 10^{-3}$	$5.099 \times 10^{-5}$	99%
1000	spatial+	$5.348 \times 10^{-4}$	$6.477 \times 10^{-3}$	$4.216 \times 10^{-5}$	98%
1000	svc_mle	$3.294 \times 10^{-4}$	$6.434 \times 10^{-3}$	$4.143 \times 10^{-5}$	
1000	spline_interaction	$-9.566 \times 10^{-5}$	$6.338 \times 10^{-3}$	$4.010 \times 10^{-5}$	99%
1000	gp3	$-5.282 \times 10^{-4}$	$6.478 \times 10^{-3}$	$4.216 \times 10^{-5}$	
1000	spline3	<b><math>1.538 \times 10^{-5}</math></b>	$6.539 \times 10^{-3}$	$4.268 \times 10^{-5}$	
1000	rf	$-1.886 \times 10^{-1}$	$1.370 \times 10^{-2}$	$3.575 \times 10^{-2}$	0%
1000	BART	$-2.754 \times 10^{-3}$	$1.340 \times 10^{-2}$	$1.868 \times 10^{-4}$	100%
1000	DML_gp3	$-2.531 \times 10^{-4}$	$6.690 \times 10^{-3}$	$4.473 \times 10^{-5}$	
1000	DML_spline	$1.424 \times 10^{-4}$	$6.749 \times 10^{-3}$	$4.548 \times 10^{-5}$	
1000	DML_BART	$-1.811 \times 10^{-3}$	$1.350 \times 10^{-2}$	$1.850 \times 10^{-4}$	100%
10,000	RSR	$7.715 \times 10^{-2}$	$5.237 \times 10^{-3}$	$5.980 \times 10^{-3}$	0%
10,000	spline	$-2.203 \times 10^{-4}$	$1.914 \times 10^{-3}$	$3.696 \times 10^{-6}$	96%
10,000	gp	$-1.842 \times 10^{-4}$	$1.978 \times 10^{-3}$	$3.932 \times 10^{-6}$	96%
10,000	gSEM	<b><math>3.427 \times 10^{-6}</math></b>	$1.934 \times 10^{-3}$	$3.724 \times 10^{-6}$	98%
10,000	spatial+	$-1.298 \times 10^{-4}$	$1.912 \times 10^{-3}$	<b><math>3.657 \times 10^{-6}</math></b>	97%
10,000	spline_interaction	$-2.171 \times 10^{-4}$	$1.911 \times 10^{-3}$	$3.684 \times 10^{-6}$	97%
10,000	spline3	$-1.965 \times 10^{-4}$	$1.935 \times 10^{-3}$	$3.768 \times 10^{-6}$	
10,000	rf	$-9.426 \times 10^{-2}$	$4.410 \times 10^{-3}$	$8.904 \times 10^{-3}$	0%
10,000	BART	$-8.981 \times 10^{-4}$	$2.987 \times 10^{-3}$	$9.694 \times 10^{-6}$	98%
10,000	DML_spline	$-1.965 \times 10^{-4}$	$1.991 \times 10^{-3}$	$3.987 \times 10^{-6}$	
10,000	DML_BART	$-3.668 \times 10^{-4}$	$2.992 \times 10^{-3}$	$9.053 \times 10^{-6}$	98%

TABLE 1  
*Simulation results in the linear confounding scenario*

for random forest. We will see the random forest performs poorly in most scenarios, apparently due to inappropriate flattening of estimated outcomes at the extremes of exposure values. While random forest is typically a good prediction algorithm, we caution against off-the-shelf use for counterfactual inference [72, 43].

### 6.3.2 Simple effect

$$\begin{aligned}
 S^a, S^b &\sim_{iid} \text{unif}(-1, 1) \\
 U &= \sin(2\pi S^a * S^b) + S^a + S^b \\
 X &\sim N(U^3, 5) \\
 Y &\sim N(3U + X, 1)
 \end{aligned}$$

### 6.3.3 Nonlinear effect

$$\begin{aligned}
 S^a, S^b &\sim_{iid} \text{unif}(-1, 1) \\
 U &= \sin(2\pi S^a * S^b) + S^a + S^b \\
 X &\sim N(U^3, 5)
 \end{aligned}$$

$$Y \sim N(3U + X + X^2, 1)$$

Only the flexible models are correctly specified in the nonlinear effect scenario, Table 3; all other methods exhibit substantial bias. Only the BART methods have good confidence interval coverage. For both sample sizes, DML\_BART has the lowest bias, and use of DML improves on the bias of each machine learning algorithm.

### 6.3.4 Random heterogeneous effect

$$\begin{aligned}
 S^a, S^b &\sim_{iid} \text{unif}(-1, 1) \\
 U &= \sin(2\pi S^a * S^b) + S^a + S^b \\
 X &\sim N(U^3, 5 * \exp(U/2)) \\
 d &\sim N(0, 1) \\
 Y &\sim N(U + (1 + d) * X, 1)
 \end{aligned}$$

In the random heterogeneous effect scenario, Table 4, no model is correctly specified since the effect varies in a way that is not a well-behaved function of space. However, the randomness in the heterogeneity avoids most estimation bias; it is rather the variance of the methods that

n	method	bias	sd	mse	coverage
1000	RSR	$2.589 \times 10^{-1}$	$1.528 \times 10^{-2}$	$6.727 \times 10^{-2}$	0%
1000	spline	$6.863 \times 10^{-3}$	$6.502 \times 10^{-3}$	$8.930 \times 10^{-5}$	81%
1000	gp	$7.727 \times 10^{-3}$	$6.770 \times 10^{-3}$	$1.054 \times 10^{-4}$	76%
1000	gSEM	$7.305 \times 10^{-2}$	$7.584 \times 10^{-3}$	$5.394 \times 10^{-3}$	0%
1000	spatial+	$1.084 \times 10^{-2}$	$6.826 \times 10^{-3}$	$1.641 \times 10^{-4}$	73%
1000	svc_mle	$7.387 \times 10^{-3}$	$6.855 \times 10^{-3}$	$1.015 \times 10^{-4}$	
1000	spline_interaction	$6.801 \times 10^{-3}$	$6.568 \times 10^{-3}$	$8.930 \times 10^{-5}$	96%
1000	gp3	$2.682 \times 10^{-3}$	$6.939 \times 10^{-3}$	$5.524 \times 10^{-5}$	
1000	spline3	$6.308 \times 10^{-2}$	$4.068 \times 10^{-2}$	$5.631 \times 10^{-3}$	
1000	rf	$-1.458 \times 10^{-1}$	$1.595 \times 10^{-2}$	$2.152 \times 10^{-2}$	0%
1000	BART	$7.672 \times 10^{-3}$	$1.680 \times 10^{-2}$	$3.405 \times 10^{-4}$	100%
1000	DML_gp3	<b><math>1.396 \times 10^{-3}</math></b>	$7.065 \times 10^{-3}$	<b><math>5.177 \times 10^{-5}</math></b>	
1000	DML_spline	$2.998 \times 10^{-2}$	$3.476 \times 10^{-2}$	$2.104 \times 10^{-3}$	
1000	DML_BART	$3.432 \times 10^{-3}$	$1.685 \times 10^{-2}$	$2.950 \times 10^{-4}$	100%
10,000	RSR	$2.580 \times 10^{-1}$	$4.749 \times 10^{-3}$	$6.661 \times 10^{-2}$	0%
10,000	spline	$1.630 \times 10^{-3}$	$1.947 \times 10^{-3}$	$6.433 \times 10^{-6}$	86%
10,000	gp	$2.159 \times 10^{-3}$	$1.990 \times 10^{-3}$	$8.605 \times 10^{-6}$	81%
10,000	gSEM	$1.564 \times 10^{-2}$	$2.089 \times 10^{-3}$	$2.488 \times 10^{-4}$	0%
10,000	spatial+	$5.063 \times 10^{-4}$	$1.958 \times 10^{-3}$	<b><math>4.075 \times 10^{-6}</math></b>	96%
10,000	spline_interaction	$1.614 \times 10^{-3}$	$1.945 \times 10^{-3}$	$6.372 \times 10^{-6}$	88%
10,000	spline3	$2.244 \times 10^{-2}$	$6.780 \times 10^{-3}$	$5.495 \times 10^{-4}$	
10,000	rf	$-7.677 \times 10^{-2}$	$4.497 \times 10^{-3}$	$5.914 \times 10^{-3}$	0%
10,000	BART	$2.642 \times 10^{-3}$	$3.618 \times 10^{-3}$	$2.002 \times 10^{-5}$	97%
10,000	DML_spline	$6.870 \times 10^{-3}$	$7.080 \times 10^{-3}$	$9.712 \times 10^{-5}$	
10,000	DML_BART	<b><math>4.626 \times 10^{-4}</math></b>	$3.586 \times 10^{-3}$	$1.302 \times 10^{-5}$	100%

TABLE 2  
*Simulation results in the simple effect scenario*

are increased relative to the simple effect scenario. The DML\_BART method has the lowest bias for each sample size, while spatially-varying coefficient models have the lowest MSE. Use of DML improves on the bias of each machine learning algorithm.

### 6.3.5 Noisy confounding

$$S^a, S^b \sim_{iid} \text{unif}(-1, 1)$$

$$U \sim N(\sin(2\pi S^a * S^b) + S^a + S^b, 1)$$

$$X \sim N(U^3, 5)$$

$$Y \sim N(5U + X, 1)$$

In the noisy confounding scenario, Table 5, no method is capable of controlling for the confounding surface because it is not a measurable function of spatial location. All models exhibit substantial error.

### 6.3.6 Less noisy confounding

$$S^a, S^b \sim_{iid} \text{unif}(-1, 1)$$

$$U \sim N(\sin(2\pi S^a * S^b) + S^a + S^b, 0.1)$$

$$X \sim N(U^3, 5)$$

$$Y \sim N(5U + X, 1)$$

In the less noisy confounding scenario, Table 6, all models are still misspecified, though the smaller departure from smooth confounding allows reasonable estimates, with results more similar to the simple effect scenario.

### 6.3.7 Smooth exposure

$$S^a, S^b \sim_{iid} \text{unif}(-1, 1)$$

$$U = \sin(2\pi S^a * S^b) + S^a + S^b$$

$$X = C^3 + \cos(2\pi S^a * S^b)$$

$$Y \sim N(3C + X, 1)$$

When the exposure is a perfectly smooth function of spatial location, 7, just as the unmeasured confounder is, their effects cannot be disentangled by any of the models;

n	method	bias	sd	mse	coverage
1000	RSR	$-2.791 \times 10^0$	$1.065 \times 10^0$	$8.921 \times 10^0$	0%
1000	spline	$-1.157 \times 10^0$	$6.826 \times 10^{-1}$	$1.804 \times 10^0$	25%
1000	gp	$-1.322 \times 10^0$	$6.891 \times 10^{-1}$	$2.221 \times 10^0$	17%
1000	gSEM	$-1.254 \times 10^0$	$7.258 \times 10^{-1}$	$2.098 \times 10^0$	55%
1000	spatial+	$-1.087 \times 10^0$	$6.927 \times 10^{-1}$	$1.661 \times 10^0$	63%
1000	svc_mle	$-1.145 \times 10^0$	$2.002 \times 10^{-1}$	$1.350 \times 10^0$	
1000	spline_interaction	$-9.852 \times 10^{-1}$	$4.471 \times 10^{-1}$	$1.170 \times 10^0$	38%
1000	gp3	$3.652 \times 10^{-2}$	$3.773 \times 10^{-1}$	$1.434 \times 10^{-1}$	
1000	spline3	$8.767 \times 10^{-2}$	$3.791 \times 10^{-1}$	$1.511 \times 10^{-1}$	
1000	rf	$-3.678 \times 10^{-1}$	$3.409 \times 10^{-1}$	$2.513 \times 10^{-1}$	75%
1000	BART	$2.818 \times 10^{-2}$	$3.902 \times 10^{-1}$	$1.527 \times 10^{-1}$	98%
1000	DML_gp3	$2.911 \times 10^{-2}$	$3.771 \times 10^{-1}$	<b><math>1.428 \times 10^{-1}</math></b>	
1000	DML_spline	$5.456 \times 10^{-2}$	$3.765 \times 10^{-1}$	$1.444 \times 10^{-1}$	
1000	DML_BART	<b><math>4.759 \times 10^{-3}</math></b>	$3.901 \times 10^{-1}$	$1.519 \times 10^{-1}$	98%
10,000	RSR	$-2.853 \times 10^0$	$3.774 \times 10^{-1}$	$8.283 \times 10^0$	0%
10,000	spline	$-1.061 \times 10^0$	$2.014 \times 10^{-1}$	$1.166 \times 10^0$	0%
10,000	gp	$-1.084 \times 10^0$	$2.010 \times 10^{-1}$	$1.215 \times 10^0$	0%
10,000	gSEM	$-1.146 \times 10^0$	$2.053 \times 10^{-1}$	$1.356 \times 10^0$	0%
10,000	spatial+	$-1.042 \times 10^0$	$2.014 \times 10^{-1}$	$1.126 \times 10^0$	0%
10,000	spline_interaction	$-9.893 \times 10^{-1}$	$1.594 \times 10^{-1}$	$1.004 \times 10^0$	0%
10,000	spline3	$2.979 \times 10^{-2}$	$1.229 \times 10^{-1}$	$1.594 \times 10^{-2}$	
10,000	rf	$-1.456 \times 10^{-1}$	$1.143 \times 10^{-1}$	$3.421 \times 10^{-2}$	75%
10,000	BART	$1.308 \times 10^{-2}$	$1.253 \times 10^{-1}$	$1.581 \times 10^{-2}$	96%
10,000	DML_spline	$1.421 \times 10^{-2}$	$1.229 \times 10^{-1}$	<b><math>1.524 \times 10^{-2}</math></b>	
10,000	DML_BART	<b><math>5.706 \times 10^{-3}</math></b>	$1.254 \times 10^{-1}$	$1.569 \times 10^{-2}$	96%

TABLE 3  
*Nonlinear effect simulation results*

this can be seen as an extreme violation of positivity. Because of this, all models exhibit substantial error. (Some of the spline-based methods exhibit decent confidence interval coverage, presumably due to computational instability in the bootstrap distribution arising from the concavity.)

*Summary of simulations* These simulations confirm multiple strands of argument from the body of the paper. First, effect heterogeneity and nonlinearity can result in severe bias in models which are unable to account for them. On the other hand, with the noted exception of random forest, flexible models perform well, even competitive with simpler models when the simpler models are correctly specified. DML methods tend to reduce bias and MSE compared to their (single) machine learning counterparts. The assumptions of smooth confounding through space and extra-spatial variation in the exposure of interest have proven to be critical, though small departures from smoothness of the confounding surface were not severely harmful.

n	method	bias	sd	mse	coverage
1000	RSR	$1.731 \times 10^{-1}$	$8.450 \times 10^{-2}$	$3.707 \times 10^{-2}$	0%
1000	spline	$2.433 \times 10^{-2}$	$8.790 \times 10^{-2}$	$8.302 \times 10^{-3}$	51%
1000	gp	$3.795 \times 10^{-2}$	$8.729 \times 10^{-2}$	$9.044 \times 10^{-3}$	51%
1000	gSEM	$5.425 \times 10^{-2}$	$9.213 \times 10^{-2}$	$1.141 \times 10^{-2}$	90%
1000	spatial+	$2.323 \times 10^{-2}$	$9.081 \times 10^{-2}$	$8.770 \times 10^{-3}$	93%
1000	svc_mle	$2.079 \times 10^{-2}$	$3.639 \times 10^{-2}$	<b><math>1.754 \times 10^{-3}</math></b>	
1000	spline_interaction	$4.651 \times 10^{-2}$	$5.233 \times 10^{-2}$	$4.896 \times 10^{-3}$	94%
1000	gp3	$1.817 \times 10^{-2}$	$1.390 \times 10^{-1}$	$1.962 \times 10^{-2}$	
1000	spline3	$4.436 \times 10^{-2}$	$2.268 \times 10^{-1}$	$5.331 \times 10^{-2}$	
1000	rf	$-1.103 \times 10^{-1}$	$5.951 \times 10^{-2}$	$1.571 \times 10^{-2}$	72%
1000	BART	$1.216 \times 10^{-2}$	$1.014 \times 10^{-1}$	$1.040 \times 10^{-2}$	100%
1000	DML_gp3	$-1.420 \times 10^{-2}$	$1.363 \times 10^{-1}$	$1.874 \times 10^{-2}$	
1000	DML_spline	$2.872 \times 10^{-2}$	$2.301 \times 10^{-1}$	$5.369 \times 10^{-2}$	
1000	DML_BART	<b><math>6.093 \times 10^{-3}</math></b>	$1.023 \times 10^{-1}$	$1.048 \times 10^{-2}$	100%
10,000	RSR	$1.760 \times 10^{-1}$	$2.928 \times 10^{-2}$	$3.184 \times 10^{-2}$	0%
10,000	spline	$1.043 \times 10^{-2}$	$2.919 \times 10^{-2}$	$9.573 \times 10^{-4}$	52%
10,000	gp	$2.034 \times 10^{-2}$	$2.946 \times 10^{-2}$	$1.278 \times 10^{-3}$	47%
10,000	gSEM	$1.407 \times 10^{-2}$	$2.939 \times 10^{-2}$	$1.058 \times 10^{-3}$	90%
10,000	spatial+	$5.516 \times 10^{-3}$	$2.923 \times 10^{-2}$	$8.816 \times 10^{-4}$	93%
10,000	spline_interaction	$2.210 \times 10^{-2}$	$1.800 \times 10^{-2}$	<b><math>8.110 \times 10^{-4}</math></b>	80%
10,000	spline3	$4.608 \times 10^{-2}$	$2.875 \times 10^{-2}$	$2.947 \times 10^{-3}$	
10,000	rf	$-5.237 \times 10^{-2}$	$2.216 \times 10^{-2}$	$3.231 \times 10^{-3}$	62%
10,000	BART	$1.036 \times 10^{-2}$	$3.330 \times 10^{-2}$	$1.212 \times 10^{-3}$	100%
10,000	DML_spline	$1.740 \times 10^{-2}$	$3.327 \times 10^{-2}$	$1.405 \times 10^{-3}$	
10,000	DML_BART	<b><math>1.913 \times 10^{-3}</math></b>	$3.456 \times 10^{-2}$	$1.193 \times 10^{-3}$	100%

TABLE 4  
*Random heterogeneous effect simulation results*

n	method	bias	sd	mse	coverage
1000	RSR	$4.240 \times 10^{-1}$	$3.038 \times 10^{-2}$	$1.807 \times 10^{-1}$	0%
1000	spline	$2.979 \times 10^{-1}$	$2.432 \times 10^{-2}$	$8.936 \times 10^{-2}$	0%
1000	gp	$3.004 \times 10^{-1}$	$2.442 \times 10^{-2}$	$9.086 \times 10^{-2}$	0%
1000	gSEM	$3.521 \times 10^{-1}$	$2.521 \times 10^{-2}$	$1.246 \times 10^{-1}$	0%
1000	spatial+	$3.055 \times 10^{-1}$	$2.443 \times 10^{-2}$	$9.391 \times 10^{-2}$	0%
1000	svc_mle	$3.397 \times 10^{-1}$	$2.318 \times 10^{-2}$	$1.160 \times 10^{-1}$	
1000	spline_interaction	$3.436 \times 10^{-1}$	$1.890 \times 10^{-2}$	$1.184 \times 10^{-1}$	0%
1000	gp3	$3.753 \times 10^{-1}$	$2.096 \times 10^{-2}$	$1.413 \times 10^{-1}$	
1000	spline3	$4.230 \times 10^{-1}$	$2.279 \times 10^{-2}$	$1.795 \times 10^{-1}$	
1000	rf	<b><math>1.072 \times 10^{-1}</math></b>	$3.980 \times 10^{-2}$	<b><math>1.308 \times 10^{-2}</math></b>	49%
1000	BART	$3.278 \times 10^{-1}$	$5.504 \times 10^{-2}$	$1.105 \times 10^{-1}$	0%
1000	DML_gp3	$3.572 \times 10^{-1}$	$2.244 \times 10^{-2}$	$1.281 \times 10^{-1}$	
1000	DML_spline	$3.324 \times 10^{-1}$	$2.567 \times 10^{-2}$	$1.111 \times 10^{-1}$	
1000	DML_BART	$3.204 \times 10^{-1}$	$5.549 \times 10^{-2}$	$1.057 \times 10^{-1}$	0%
10,000	RSR	$4.197 \times 10^{-1}$	$1.015 \times 10^{-2}$	$1.763 \times 10^{-1}$	0%
10,000	spline	$2.879 \times 10^{-1}$	$7.850 \times 10^{-3}$	$8.295 \times 10^{-2}$	0%
10,000	gp	$2.880 \times 10^{-1}$	$7.820 \times 10^{-3}$	$8.299 \times 10^{-2}$	0%
10,000	gSEM	$3.007 \times 10^{-1}$	$8.043 \times 10^{-3}$	$9.051 \times 10^{-2}$	0%
10,000	spatial+	$2.879 \times 10^{-1}$	$7.798 \times 10^{-3}$	$8.296 \times 10^{-2}$	0%
10,000	spline_interaction	$3.443 \times 10^{-1}$	$5.832 \times 10^{-3}$	$1.186 \times 10^{-1}$	0%
10,000	spline3	$3.678 \times 10^{-1}$	$1.214 \times 10^{-2}$	$1.354 \times 10^{-1}$	
10,000	rf	<b><math>2.182 \times 10^{-1}</math></b>	$1.239 \times 10^{-2}$	<b><math>4.775 \times 10^{-2}</math></b>	0%
10,000	BART	$3.194 \times 10^{-1}$	$2.167 \times 10^{-2}$	$1.025 \times 10^{-1}$	0%
10,000	DML_spline	$3.373 \times 10^{-1}$	$1.202 \times 10^{-2}$	$1.139 \times 10^{-1}$	
10,000	DML_BART	$3.255 \times 10^{-1}$	$2.052 \times 10^{-2}$	$1.064 \times 10^{-1}$	0%

TABLE 5  
Noisy confounding simulation results

n	method	bias	sd	mse	coverage
1000	RSR	$4.338 \times 10^{-1}$	$2.410 \times 10^{-2}$	$1.888 \times 10^{-1}$	0%
1000	spline	$1.421 \times 10^{-2}$	$7.492 \times 10^{-3}$	$2.581 \times 10^{-4}$	49%
1000	gp	$1.464 \times 10^{-2}$	$7.791 \times 10^{-3}$	$2.748 \times 10^{-4}$	49%
1000	gSEM	$9.108 \times 10^{-2}$	$9.040 \times 10^{-3}$	$8.378 \times 10^{-3}$	0%
1000	spatial+	$1.768 \times 10^{-2}$	$7.902 \times 10^{-3}$	$3.750 \times 10^{-4}$	45%
1000	svc_mle	$1.401 \times 10^{-2}$	$7.693 \times 10^{-3}$	$2.553 \times 10^{-4}$	
1000	spline_interaction	$1.403 \times 10^{-2}$	$7.515 \times 10^{-3}$	$2.532 \times 10^{-4}$	81%
1000	gp3	$8.156 \times 10^{-3}$	$7.658 \times 10^{-3}$	$1.251 \times 10^{-4}$	
1000	spline3	$9.351 \times 10^{-2}$	$6.410 \times 10^{-2}$	$1.284 \times 10^{-2}$	
1000	rf	$-1.034 \times 10^{-1}$	$2.001 \times 10^{-2}$	$1.109 \times 10^{-2}$	2%
1000	BART	$1.608 \times 10^{-2}$	$1.896 \times 10^{-2}$	$6.173 \times 10^{-4}$	100%
1000	DML_gp3	<b><math>7.789 \times 10^{-3}</math></b>	$7.932 \times 10^{-3}$	<b><math>1.235 \times 10^{-4}</math></b>	
1000	DML_spline	$5.611 \times 10^{-2}$	$5.497 \times 10^{-2}$	$6.164 \times 10^{-3}$	
1000	DML_BART	$1.143 \times 10^{-2}$	$1.889 \times 10^{-2}$	$4.865 \times 10^{-4}$	100%
10,000	RSR	$4.334 \times 10^{-1}$	$7.335 \times 10^{-3}$	$1.879 \times 10^{-1}$	0%
10,000	spline	$8.398 \times 10^{-3}$	$2.300 \times 10^{-3}$	$7.579 \times 10^{-5}$	6%
10,000	gp	$9.312 \times 10^{-3}$	$2.298 \times 10^{-3}$	$9.197 \times 10^{-5}$	2%
10,000	gSEM	$2.439 \times 10^{-2}$	$2.461 \times 10^{-3}$	$6.009 \times 10^{-4}$	0%
10,000	spatial+	$7.380 \times 10^{-3}$	$2.299 \times 10^{-3}$	$5.973 \times 10^{-5}$	11%
10,000	spline_interaction	$8.209 \times 10^{-3}$	$2.306 \times 10^{-3}$	$7.269 \times 10^{-5}$	7%
10,000	spline3	$4.054 \times 10^{-2}$	$1.026 \times 10^{-2}$	$1.748 \times 10^{-3}$	
10,000	rf	$-5.936 \times 10^{-2}$	$5.370 \times 10^{-3}$	$3.553 \times 10^{-3}$	0%
10,000	BART	$8.915 \times 10^{-3}$	$3.818 \times 10^{-3}$	$9.399 \times 10^{-5}$	64%
10,000	DML_spline	$1.824 \times 10^{-2}$	$1.001 \times 10^{-2}$	$4.325 \times 10^{-4}$	
10,000	DML_BART	<b><math>6.480 \times 10^{-3}</math></b>	$3.778 \times 10^{-3}$	<b><math>5.621 \times 10^{-5}</math></b>	84%

TABLE 6  
*Less noisy confounding simulation results*

n	method	bias	sd	mse	coverage
1000	RSR	$6.784 \times 10^{-1}$	$3.030 \times 10^{-2}$	$4.611 \times 10^{-1}$	0%
1000	spline	$2.763 \times 10^{-1}$	$2.757 \times 10^{-2}$	<b><math>7.712 \times 10^{-2}</math></b>	0%
1000	gp	$3.755 \times 10^{-1}$	$2.176 \times 10^{-2}$	$1.415 \times 10^{-1}$	0%
1000	gSEM	$5.868 \times 10^{-1}$	$3.014 \times 10^{-1}$	$4.350 \times 10^{-1}$	73%
1000	spatial+	<b><math>2.448 \times 10^{-1}</math></b>	$3.007 \times 10^{-1}$	$1.502 \times 10^{-1}$	94%
1000	svc_mle	$3.640 \times 10^{-1}$	$4.203 \times 10^{-2}$	$1.342 \times 10^{-1}$	
1000	spline_interaction	$3.513 \times 10^{-1}$	$6.681 \times 10^{-2}$	$1.279 \times 10^{-1}$	99%
1000	gp3	$5.565 \times 10^{-1}$	$8.876 \times 10^{-2}$	$3.175 \times 10^{-1}$	
1000	spline3	$1.153 \times 10^0$	$1.582 \times 10^{-1}$	$1.353 \times 10^0$	
1000	rf	$5.394 \times 10^{-1}$	$8.793 \times 10^{-2}$	$2.986 \times 10^{-1}$	0%
1000	BART	$7.024 \times 10^{-1}$	$1.265 \times 10^{-1}$	$5.093 \times 10^{-1}$	1%
10,000	RSR	$6.750 \times 10^{-1}$	$9.106 \times 10^{-3}$	$4.557 \times 10^{-1}$	0%
10,000	spline	$2.267 \times 10^{-1}$	$1.188 \times 10^{-2}$	$5.152 \times 10^{-2}$	0%
10,000	gp	$3.229 \times 10^{-1}$	$7.812 \times 10^{-3}$	$1.043 \times 10^{-1}$	0%
10,000	gSEM	$2.386 \times 10^{-1}$	$7.345 \times 10^{-2}$	$6.231 \times 10^{-2}$	10%
10,000	spatial+	<b><math>2.049 \times 10^{-1}</math></b>	$7.285 \times 10^{-2}$	<b><math>4.726 \times 10^{-2}</math></b>	20%
10,000	spline_interaction	$3.150 \times 10^{-1}$	$4.915 \times 10^{-2}$	$1.016 \times 10^{-1}$	98%
10,000	spline3	$1.292 \times 10^0$	$9.115 \times 10^{-2}$	$1.676 \times 10^0$	
10,000	rf	$5.344 \times 10^{-1}$	$3.208 \times 10^{-2}$	$2.867 \times 10^{-1}$	0%
10,000	BART	$5.844 \times 10^{-1}$	$6.789 \times 10^{-2}$	$3.461 \times 10^{-1}$	0%

TABLE 7  
*Smooth exposure simulation results*

## 7. APPLICATION

Although the nature of the causal pathway is debated, birthweight has been widely studied for its strong correlation with health and economic outcomes in childhood and adulthood [75, 4, 11]; low birthweight is a risk factor for adverse outcomes including mortality. In addition, evidence suggests that exposure to ambient PM<sub>2.5</sub> during pregnancy is linked to reductions in birthweight [44, 3]. A 2021 meta-analysis gave an estimated  $-27.55\text{ g}$  [95% CI: (-48.45, -6.65)] change in birthweight for each  $10\mu\text{g}/\text{m}^3$  additional concentration of exposure to PM<sub>2.5</sub> during pregnancy, noting a wide range of previous effect estimates in the literature, all of which appear to derive from linear models [70].

In order to estimate the causal effect of ambient PM<sub>2.5</sub> on birthweight, it is necessary to adjust for confounding variables. “Greenspace” is a term with multiple definitions but generally refers to vegetation and natural spaces in residential environments[65]. The positive association between greenspace and birthweight has been studied [69, 14], as has the potential mitigation of PM<sub>2.5</sub> by greenspace [8]. Therefore, greenspace is a potential confounder of the relationship between PM<sub>2.5</sub> exposure and birthweight. Since greenspace is a relatively smooth function of spatial location (i.e., nearby locations have similar levels of greenspace), we may attempt to control for greenspace by controlling for spatial location.

For the present study, we use records of births from the California Department of Public Health’s Birth Statistical Master Files with mother’s home addresses geocoded using ArcGIS; we restrict our analysis to conceptions in the year 2013. We obtain daily PM<sub>2.5</sub> levels at 1 kilometer resolution from the NASA Socioeconomic Data and Applications Center [18]. To measure greenspace, we use peak normalized difference vegetation index (NDVI) measured at the census block level from the year 2013. In all our analyses, we include the potential confounding variables: race/ethnicity, parity, Kotelchuck index, maternal age, and maternal education. We exclude individuals with missing data, as well as pregnancies with recorded gestational lengths less than 22 weeks or greater than 44 weeks, mothers with recorded ages less than 15 or greater than 49, and birthweights recorded below 500 grams. This leaves us with  $n = 457,439$  live births. Latitude and longitude were recorded in the Web Mercator projection, and all quantitative variables were normalized prior to model-fitting.

We fit four families of models with four different covariate sets. The covariate sets differ by the inclusion of NDVI and/or spatial location. The fitting methods are:

- Linear/GAM: All variables (including exposure) enter the model linearly, except for spatial location, on which we put a smooth term. Only an outcome model is fit.

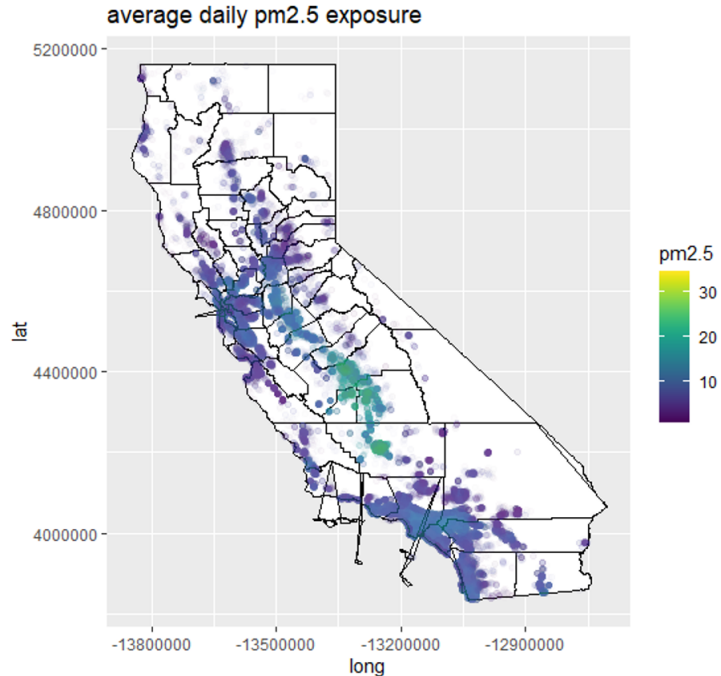


FIG 2. Location of study subjects and average daily PM<sub>2.5</sub> concentrations in 2013. Latitude and longitude are in the Web Mercator projection.

- Non-linear/GAM: Both exposure and spatial location enter the model through smooth terms; all other variables enter the model linearly. Estimate is DML.
- BART: BART is used to fit both the outcome and exposure model in the DML framework.
- BART - smooth: Same as BART model, but spatial locations are replaced with the value of the estimated spatial smooth from the non-linear GAM spatial outcome model.

The exposure shift of interest is  $0.1\text{ }\mu\text{g}/\text{m}^3$ . We choose this small shift due to a lack of positivity for larger shifts. Under linearity this effect can be multiplied by 10 in order to recover the implied average effect of a  $0.1\text{ }\mu\text{g}/\text{m}^3$  shift in exposure, and if the effect of exposure is approximately locally linear this rescaling is likely to provide a reasonable approximation. Because  $0.1\text{ }\mu\text{g}/\text{m}^3$  is too small of an effect to be of policy relevance we recommend rescaling. After rescaling the values we obtain may be compared to the results of linear models (by appropriate rescaling), but the effective interpretation of the coefficients of those linear models relies on the assumption of effect linearity which we do not make for non-linear models. Except for the linear models, 95% confidence intervals are by bootstrap standard errors. Our estimates are recorded in Table 8.

Beginning with the linear effect models, we see that the effect of adjusting for NDVI is similar to the effect of ad-

Method	Adjustment	Estimate
Linear/GAM	Neither	-0.14 (-0.18, -0.09)
Linear/GAM	NDVI	-0.11 (-0.15, -0.06)
Linear/GAM	Spatial location	-0.10 (-0.17, -0.03)
Linear/GAM	Both	-0.09 (-0.16, -0.02)
Non-linear/GAM (DML)	Neither	-0.42 (-0.49, -0.34)
Non-linear/GAM (DML)	NDVI	-0.35 (-0.43, -0.28)
Non-linear/GAM (DML)	Spatial location	-0.14 (-0.24, -0.04)
Non-linear/GAM (DML)	Both	-0.15 (-0.26, -0.05)
BART (DML)	Neither	-0.43 (-0.51, -0.34)
BART (DML)	NDVI	-0.35 (-0.45, -0.25)
BART - smooth (DML)	Spatial location*	-0.30 (-0.42, -0.18)
BART - smooth (DML)	Both*	-0.16 (-0.28, -0.03)

TABLE 8

Estimated effects of a  $0.1\mu\text{g}/\text{m}^3$  shift in average daily PM<sub>2.5</sub> exposure on birthweight in grams. An asterisk indicates that the estimated smooth from the GAM model was used for adjustment in place of directly using the spatial location.

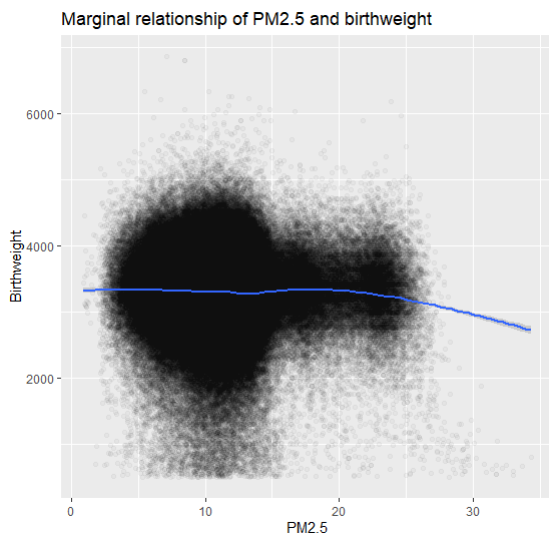


FIG 3. Scatterplot of average daily PM<sub>2.5</sub> concentration exposure in  $\mu\text{g}/\text{m}^3$  and birthweight in grams.

justing for spatial location. This is consistent with the understanding that spatial location stands in for the unmeasured confounder NDVI.

However, an assumption of linear effect may not be consistent with the data. As we can see from Figure 3, there appears to be a threshold effect where an effect only appears at high levels of exposure.

The non-linear effect GAM models assume a homogeneous effect but do not assume the effect is linear. The estimates from these models are different from those of the linear effect models, but they display similar pattern by which adjusting for spatial location and NDVI has a

qualitatively similar effect. However, adjusting for spatial location decreases the magnitude of the estimated effect by more than adjusting for NDVI, suggesting that adjusting for space "picks up" additional confounding variables.

We also fit BART models which assume neither homogeneity or linearity. The non-spatial estimates (Adjustment: Neither or NDVI) are very similar to the non-linear GAM estimates, but the models which adjust for space (not shown) were aberrant, suggesting a much *larger* effect magnitude. We believe that in this scenario, the BART model was incapable of learning the appropriate adjustment for space; perhaps the inclusion of a larger set of covariates makes this model fitting more difficult. In addition, the large sample size makes posterior sampling computationally difficult, and the estimates may be prone to Monte Carlo error. The BART - smooth model is our attempt at a compromise, in which a BART model is fit using the estimated functional smooth from the Non-linear/GAM spatial outcome model rather than spatial location itself. That is, while BART is incapable of adjusting for the raw spatial location, it may yield reasonable estimates if fed the smooth term estimated from the GAM model. (We write the adjustment sets for these models with an asterisk to denote this distinction.) We do in fact observe the BART - smooth estimates to be much more similar to the non-linear/GAM estimates.

We believe the most reliable estimates are those that come from non-linear models while controlling for all known covariates. These estimates are  $-0.15(-0.26, -0.05)$  from the Non-linear/GAM model and  $-0.16(-0.28, -0.03)$  from the BART - smooth model. These estimates are concordant with each other as well as the confidence interval

given by the [70] meta-analysis of  $(-48.45, -6.65)$  for a  $10 \mu\text{g}/\text{m}^3$  increase.

Given that multiple models were fit in an experimental manner, these results should be seen as exploratory and suggestive rather than as a definite contribution to the scientific literature on environmental exposures during pregnancy. Other limitations include the potential impact of “live-birth bias” (the bias arising from only including data from live births, analogous to the “birthweight paradox” concerning conditioning on low birth weight) [29, 35], and the mismatch in measurement resolution of various covariates, including NDVI and  $\text{PM}_{2.5}$ .

## 8. DISCUSSION

In this paper, we have argued that spatial confounding can be understood most clearly as omitted variable bias. We have given conditions sufficient for the identification and estimation of causal effects when unmeasured confounders vary spatially. The most basic assumption is there should not be nonspatial variation in the unmeasured confounder; if there is then the methods described in this paper may mitigate, but would not be expected to fully control for, confounding bias. We recommend the use of flexible models to estimate causal effects rather than the restrictive (partially) linear models that are typically used in spatial statistics; the assumptions of linearity and homogeneity are often implausible in practice and can lead to substantial bias. DML methods should be considered strong candidates for spatial models, though our data analysis shows this application should be handled with care.

There remains much room for further research. For example, unmeasured confounders will often be associated with spatial location even if they are not measurable functions of spatial location. In this scenario, it would be beneficial to quantify the extent to which confounding bias can be reduced by including spatial location in the causal model and/or provide a framework for sensitivity analysis for causal estimates. The assessment of exposures that are perfectly smooth in space (for example, distance to some location such as a factory) is beyond the reach of our current methods due to violation of positivity but may be possible under certain assumptions about relevant scales of variation, as in [50] and [37]. In addition, the mitigation of spatial confounding for areal data has been mostly ignored in this work as some fundamental concepts are distinct in the areal domain; with discrete locations, it is not possible for a confounding variable to be a smooth function, and it is not obvious how to consider an asymptotic regime as the number of areal units is typically fixed.

## REFERENCES

- [1] ANGRIST, J. (2003). Treatment Effect Heterogeneity in Theory and Practice Working Paper No. 9708, National Bureau of Economic Research.
- [2] BANERJEE, S., GELFAND, A. E., FINLEY, A. O. and SANG, H. (2008). Gaussian predictive process models for large spatial data sets. *Journal of the Royal Statistical Society. Series B (Statistical Methodology)* **70** 825–848. <https://doi.org/10.1111/j.1467-9868.2008.00663.x>
- [3] BASU, R., HARRIS, M., SIE, L., MALIG, B., BROADWIN, R. and GREEN, R. (2014). Effects of fine particulate matter and its constituents on low birth weight among full-term infants in California. *Environmental Research* **128** 42–51. <https://doi.org/10.1016/j.envres.2013.10.008>
- [4] BEHRMAN, J. R. and ROSENZWEIG, M. R. (2004). Returns to Birthweight. *The Review of Economics and Statistics* **86** 586–601. <https://doi.org/10.1162/003465304323031139>
- [5] BENKESER, D., CARONE, M., LAAN, M. J. V. D. and GILBERT, P. B. (2017). Doubly robust nonparametric inference on the average treatment effect. *Biometrika* **104** 863–880. <https://doi.org/10.1093/biomet/asx053>
- [6] BESAG, J. (1974). Spatial Interaction and the Statistical Analysis of Lattice Systems. *Journal of the Royal Statistical Society. Series B (Methodological)* **36** 192–236.
- [7] BREIMAN, L. (2001). Random forests. *Machine Learning* **45** 5–32. <https://doi.org/10.1023/a:1010933404324>
- [8] CHEN, M., DAI, F., YANG, B. and ZHU, S. (2019). Effects of neighborhood green space on  $\text{PM}_{2.5}$  mitigation: Evidence from five megacities in China. *Building and Environment* **156** 33–45. <https://doi.org/10.1016/j.buildenv.2019.03.007>
- [9] CHERNOZHUKOV, V., CHETVERIKOV, D., DEMIRER, M., DUFLO, E., HANSEN, C., NEWHEY, W. and ROBINS, J. (2018). Double/debiased machine learning for treatment and structural parameters. *The Econometrics Journal* **21** C1-C68. <https://doi.org/10.1111/ectj.12097>
- [10] CHIPMAN, H. A., GEORGE, E. I. and MCCULLOCH, R. E. (2010). BART: Bayesian additive regression trees. *The Annals of Applied Statistics* **4** 266 – 298. <https://doi.org/10.1214/09-AOAS285>
- [11] CHYE, J. and LIM, C. (1999). Very low birth weight infants–mortality and predictive risk factors. *Singapore medical journal* **40** 565–570.
- [12] COX, C. (1987). Threshold Dose-Response Models in Toxicology. *Biometrics* **43** 511–523.
- [13] CRESSIE, N. A. C. (1993). *Statistics for Spatial Data*. John Wiley & Sons, Inc. <https://doi.org/10.1002/9781119115151>
- [14] CUSACK, L., LARKIN, A., CAROZZA, S. E. and HYSTAD, P. (2017). Associations between multiple green space measures and birth weight across two US cities. *Health Place* **47** 36–43. <https://doi.org/10.1016/j.healthplace.2017.07.002>
- [15] DAMBON, J. A., SIGRIST, F. and FURRER, R. (2021). Maximum likelihood estimation of spatially varying coefficient models for large data with an application to real estate price prediction. *Spatial Statistics* **41** 100470. <https://doi.org/10.1016/j.spasta.2020.100470>
- [16] DAMBON, J. A., SIGRIST, F. and FURRER, R. (2021). *varycoef*: Modeling Spatially Varying Coefficients.
- [17] D'AMOUR, A., DING, P., FELLER, A., LEI, L. and SEKHON, J. (2021). Overlap in observational studies with high-dimensional covariates. *Journal of Econometrics* **221** 644–654. <https://doi.org/10.1016/j.jeconom.2019.10.014>
- [18] DI, Q., WEI, Y., SHTEIN, A., HULTQUIST, C., XING, X., AMINI, H., SHI, L., KLOOG, I., SILVERN, R., KELLY, J., SABATH, M. B., CHOIRAT, C., KOUTRAKIS, P., LYAPUSTIN, A., WANG, Y., MICKLEY, L. J. and SCHWARTZ, J. (2021). Daily and Annual  $\text{PM}_{2.5}$  Concentrations for the Contiguous United States, 1-km Grids, v1 (2000 - 2016). <https://doi.org/10.7927/0RVR-4538>

[19] DOMINICI, F., McDERMOTT, A. and HASTIE, T. J. (2004). Improved Semiparametric Time Series Models of Air Pollution and Mortality. *Journal of the American Statistical Association* **99** 938-948. <https://doi.org/10.1198/016214504000000656>

[20] DORIE, V. (2020). dbarts: Discrete Bayesian Additive Regression Trees Sampler. R package version 0.9-19.

[21] DUBRULE, O. (1984). Comparing splines and kriging. *Computers & Geosciences* **10** 327-338. [https://doi.org/10.1016/0098-3004\(84\)90030-X](https://doi.org/10.1016/0098-3004(84)90030-X)

[22] DUPONT, E., WOOD, S. N. and AUGUSTIN, N. (2020). Spatial+: a novel approach to spatial confounding. arXiv 2009.09420.

[23] EFRON, B. (1987). Better Bootstrap Confidence Intervals. *Journal of the American Statistical Association* **82** 171-185. <https://doi.org/10.1080/01621459.1987.10478410>

[24] ELWERT, F. and WINSHIP, C. (2014). Endogenous Selection Bias: The Problem of Conditioning on a Collider Variable. *Annual Review of Sociology* **40** 31-53. <https://doi.org/10.1146/annurev-soc-071913-043455>

[25] FAN, J. and HUANG, T. (2005). Profile likelihood inferences on semiparametric varying-coefficient partially linear models. *Bernoulli* **11**. <https://doi.org/10.3150/bj/1137421639>

[26] FUENTES, M. (2007). Approximate Likelihood for Large Irregularly Spaced Spatial Data. *Journal of the American Statistical Association* **102** 321-331. <https://doi.org/10.1198/016214506000000852>

[27] GAMERMAN, D., MOREIRA, A. R. B. and RUE, H. (2003). Space-varying regression models: specifications and simulation. *Computational Statistics & Data Analysis* **42** 513-533. [https://doi.org/10.1016/s0167-9473\(02\)00211-6](https://doi.org/10.1016/s0167-9473(02)00211-6)

[28] GELFAND, A. E., KIM, H.-J., SIRMANS, C. and BANERJEE, S. (2003). Spatial modeling with spatially varying coefficient processes. *Journal of the American Statistical Association* **98** 387-396.

[29] GOIN, D. E., CASEY, J. A., KIOUMOURTOZOGLOU, M.-A., CUSHING, L. J. and MORELLO-FROSCH, R. (2021). Environmental hazards, social inequality, and fetal loss: Implications of live-birth bias for estimation of disparities in birth outcomes. *Environmental Epidemiology* **5** e131. <https://doi.org/10.1097/ee9.0000000000000131>

[30] GOUVEIA, N. (2000). Time series analysis of air pollution and mortality: effects by cause, age and socioeconomic status. *Journal of Epidemiology & Community Health* **54** 750-755. <https://doi.org/10.1136/jech.54.10.750>

[31] GU, M., PALOMO, J. and BERGER, J. (2020). RobustGaSP: Robust Gaussian Stochastic Process Emulation R package version 0.6.1.

[32] GUAN, Y., PAGE, G. L., REICH, B. J., VENTRUCCI, M. and YANG, S. (2020). A spectral adjustment for spatial confounding.

[33] HANEUSE, S. and ROTNITZKY, A. (2013). Estimation of the effect of interventions that modify the received treatment. *Statistics in Medicine* **32** 5260-5277. <https://doi.org/10.1002/sim.5907>

[34] HANEUSE, S., VANDERWEELE, T. J. and ARTERBURN, D. (2019). Using the E-Value to Assess the Potential Effect of Unmeasured Confounding in Observational Studies. *JAMA* **321** 602. <https://doi.org/10.1001/jama.2018.21554>

[35] HERNANDEZ-DIAZ, S., SCHISTERMAN, E. F. and HERNAN, M. A. (2006). The Birth Weight "Paradox" Uncovered? *American Journal of Epidemiology* **164** 1115-1120. <https://doi.org/10.1093/aje/kwj275>

[36] HODGES, J. S. and REICH, B. J. (2010). Adding Spatially-Correlated Errors Can Mess Up the Fixed Effect You Love. *The American Statistician* **64** 325-334. <https://doi.org/10.1198/tast.2010.10052>

[37] KELLER, J. P. and SZPIRO, A. A. (2020). Selecting a scale for spatial confounding adjustment. *Journal of the Royal Statistical Society: Series A (Statistics in Society)* **183** 1121-1143. <https://doi.org/10.1111/rssa.12556>

[38] KENNEDY, E. H. (2019). Nonparametric Causal Effects Based on Incremental Propensity Score Interventions. *Journal of the American Statistical Association* **114** 645-656. <https://doi.org/10.1080/01621459.2017.1422737>

[39] KENNEDY, E. H., MA, Z., MCHUGH, M. D. and SMALL, D. S. (2017). Nonparametric methods for doubly robust estimation of continuous treatment effects. *Journal of the Royal Statistical Society: Series B (Statistical Methodology)* **79** 1229-1245.

[40] KHAN, K. and CALDER, C. A. (2020). Restricted Spatial Regression Methods: Implications for Inference. *Journal of the American Statistical Association* **0** 1-13. <https://doi.org/10.1080/01621459.2020.1788949>

[41] KUROKI, M. and PEARL, J. (2014). Measurement bias and effect restoration in causal inference. *Biometrika* **101** 423-437.

[42] LASH, T. L., VANDERWEELE, T. J. and ROTHMAN, K. J. (2020). Measurement and Measurement Error. *Modern Epidemiology*.

[43] LEI, L. and CANDÈS, E. J. (2021). Conformal Inference of Counterfactuals and Individual Treatment Effects.

[44] LI, X., HUANG, S., JIAO, A., YANG, X., YUN, J., WANG, Y., XUE, X., CHU, Y., LIU, F., LIU, Y., REN, M., CHEN, X., LI, N., LU, Y., MAO, Z., TIAN, L. and XIANG, H. (2017). Association between ambient fine particulate matter and preterm birth or term low birth weight: An updated systematic review and meta-analysis. *Environmental Pollution* **227** 596-605. <https://doi.org/10.1016/j.envpol.2017.03.055>

[45] LIAW, A. and WIENER, M. (2002). Classification and Regression by randomForest. *R News* **2** 18-22.

[46] NAIMI, A. I., MISHLER, A. E. and KENNEDY, E. H. (2020). Challenges in Obtaining Valid Causal Effect Estimates with Machine Learning Algorithms.

[47] OGBURN, E. L. and VANDERWEELE, T. J. (2012). On the non-differential misclassification of a binary confounder. *Epidemiology (Cambridge, Mass.)* **23** 433.

[48] OGBURN, E. L. and VANDERWEELE, T. J. (2013). Bias attenuation results for nondifferentially mismeasured ordinal and coarsened confounders. *Biometrika* **100** 241-248.

[49] OSAMA, M., ZACHARIAH, D. and SCHÖN, T. B. (2019). Inferring Heterogeneous Causal Effects in Presence of Spatial Confounding. In *Proceedings of the 36th International Conference on Machine Learning* (K. CHAUDHURI and R. SALAKHUTDINOV, eds.). *Proceedings of Machine Learning Research* **97** 4942-4950. PMLR.

[50] PACIOREK, C. J. (2010). The Importance of Scale for Spatial-Confounding Bias and Precision of Spatial Regression Estimators. *Statistical Science* **25** 107 - 125. <https://doi.org/10.1214/10-STS326>

[51] PAPADOGEORGOU, G., CHOIRAT, C. and ZIGLER, C. M. (2018). Adjusting for unmeasured spatial confounding with distance adjusted propensity score matching. *Biostatistics* **20** 256-272. <https://doi.org/10.1093/biostatistics/kxx074>

[52] PEÑA, J. M., BALGI, S., SJÖLANDER, A. and GABRIEL, E. E. (2021). On the bias of adjusting for a non-differentially mismeasured discrete confounder. *Journal of Causal Inference* **9** 229-249.

[53] PETERSEN, M. L., PORTER, K. E., GRUBER, S., WANG, Y. and VAN DER LAAN, M. J. (2012). Diagnosing and responding to violations in the positivity assumption. *Statistical Methods in Medical Research* **21** 31-54.

[54] PUGH, C. C. (2015). *Real mathematical analysis*. Springer, Cham.

[55] RAMSAY, T., BURNETT, R. and KREWSKI, D. (2003). Exploring bias in a generalized additive model for spatial air pollution data. *Environmental Health Perspectives* **111** 1283–1288. <https://doi.org/10.1289/ehp.6047>

[56] RICE, J. (1986). Convergence rates for partially splined models. *Statistics & Probability Letters* **4** 203–208. [https://doi.org/10.1016/0167-7152\(86\)90067-2](https://doi.org/10.1016/0167-7152(86)90067-2)

[57] RUBIN, D. B. (1974). Estimating causal effects of treatments in randomized and nonrandomized studies. *Journal of Educational Psychology* **66** 688–701. <https://doi.org/10.1037/h0037350>

[58] SAHA, A., BASU, S. and DATTA, A. (2021). Random forests for spatially dependent data. *Journal of the American Statistical Association* 1–19.

[59] SAHA, A. and DATTA, A. (2018). BRISC: bootstrap for rapid inference on spatial covariances. *Stat* **7** e184. e184 sta4.184. <https://doi.org/10.1002/sta4.184>

[60] SAHA, A. and DATTA, A. (2020). BRISC: Fast Inference for Large Spatial Datasets using BRISC R package version 0.3.0.

[61] SCHNELL, P. M. and PAPADOGEORGOU, G. (2020). Mitigating unobserved spatial confounding when estimating the effect of supermarket access on cardiovascular disease deaths. *The Annals of Applied Statistics* **14** 2069 – 2095. <https://doi.org/10.1214/20-AOAS1377>

[62] SIGRIST, F. (2020). Gaussian Process Boosting. *arXiv preprint arXiv:2004.02653*.

[63] STEIN, M. L. (2014). Limitations on low rank approximations for covariance matrices of spatial data. *Spatial Statistics* **8** 1–19. <https://doi.org/10.1016/j.spasta.2013.06.003>

[64] STUART, E. A. (2010). Matching Methods for Causal Inference: A Review and a Look Forward. *Statistical Science* **25**. <https://doi.org/10.1214/09-sts313>

[65] TAYLOR, L. and HOCHULI, D. F. (2017). Defining greenspace: Multiple uses across multiple disciplines. *Landscape and Urban Planning* **158** 25–38. <https://doi.org/10.1016/j.landurbplan.2016.09.024>

[66] TCHTGEN, E. J. T., YING, A., CUI, Y., SHI, X. and MIAO, W. (2020). An introduction to proximal causal learning. *arXiv preprint arXiv:2009.10982*.

[67] THADEN, H. and KNEIB, T. (2018). Structural Equation Models for Dealing With Spatial Confounding. *The American Statistician* **72** 239–252. <https://doi.org/10.1080/00031305.2017.1305290>

[68] TOBLER, W. R. (1970). A Computer Movie Simulating Urban Growth in the Detroit Region. *Economic Geography* **46** 234–240.

[69] TODA, M. T., MIRI, M., ALONSO, L., GÓMEZ-ROIG, M. D., FORASTER, M. and DADVAND, P. (2020). Exposure to greenspace and birth weight in a middle-income country. *Environmental Research* **189** 109866. <https://doi.org/10.1016/j.envres.2020.109866>

[70] UWAK, I., OLSON, N., FUENTES, A., MORIARTY, M., PULCZINSKI, J., LAM, J., XU, X., TAYLOR, B. D., TAIWO, S., KOEHLER, K., FOSTER, M., CHIU, W. A. and JOHNSON, N. M. (2021). Application of the navigation guide systematic review methodology to evaluate prenatal exposure to particulate matter air pollution and infant birth weight. *Environment International* **148** 106378. <https://doi.org/10.1016/j.envint.2021.106378>

[71] VANDERWEELE, T. J. and SHPITSER, I. (2013). On the definition of a confounder. *The Annals of Statistics* **41** 196–220.

[72] WAGER, S. and ATHEY, S. (2018). Estimation and Inference of Heterogeneous Treatment Effects using Random Forests. *Jour-*  
*nal of the American Statistical Association* **113** 1228–1242. <https://doi.org/10.1080/01621459.2017.1319839>

[73] WESTREICH, D. and COLE, S. R. (2010). Invited Commentary: Positivity in Practice. *American Journal of Epidemiology* **171** 674–677. <https://doi.org/10.1093/aje/kwp436>

[74] WIKLE, C. K. and HOOTEN, M. B. (2010). A general science-based framework for dynamical spatio-temporal models. *TEST* **19** 417–451. <https://doi.org/10.1007/s11749-010-0209-z>

[75] WILCOX, A. J. (2001). On the importance—and the unimportance—of birthweight. *International Journal of Epidemiology* **30** 1233–1241. <https://doi.org/10.1093/ije/30.6.1233>

[76] WOOD, S. (2003). mgcv: Mixed GAM Computation Vehicle with Automatic Smoothness Estimation.

[77] WOOD, S. N. (2003). Thin plate regression splines. *Journal of the Royal Statistical Society: Series B (Statistical Methodology)* **65** 95–114. <https://doi.org/10.1111/1467-9868.00374>

[78] YANG, Y., CHENG, G. and DUNSON, D. B. (2015). Semiparametric Bernstein-von Mises Theorem: Second Order Studies.

[79] ZIMMERMAN, D. L. and HOEF, J. M. V. (2021). On Deconfounding Spatial Confounding in Linear Models. *The American Statistician* **0** 1–9. <https://doi.org/10.1080/00031305.2021.1946149>